NASA/TM-2003-212035

Ground-Effect Characteristics of the Tu-144 Supersonic Transport Airplane

Robert E. Curry
NASA Dryden Flight Research Center
Edwards, California

Lewis R. Owens
NASA Langley Research Center
Hampton, Virginia

EC97-44203-03

October 2003

The NASA STI Program Office…in Profile

Since its founding, NASA has been dedicated to the advancement of aeronautics and space science. The NASA Scientific and Technical Information (STI) Program Office plays a key part in helping NASA maintain this important role.

The NASA STI Program Office is operated by Langley Research Center, the lead center for NASA's scientific and technical information. The NASA STI Program Office provides access to the NASA STI Database, the largest collection of aeronautical and space science STI in the world. The Program Office is also NASA's institutional mechanism for disseminating the results of its research and development activities. These results are published by NASA in the NASA STI Report Series, which includes the following report types:

- TECHNICAL PUBLICATION. Reports of completed research or a major significant phase of research that present the results of NASA programs and include extensive data or theoretical analysis. Includes compilations of significant scientific and technical data and information deemed to be of continuing reference value. NASA's counterpart of peer-reviewed formal professional papers but has less stringent limitations on manuscript length and extent of graphic presentations.

- TECHNICAL MEMORANDUM. Scientific and technical findings that are preliminary or of specialized interest, e.g., quick release reports, working papers, and bibliographies that contain minimal annotation. Does not contain extensive analysis.

- CONTRACTOR REPORT. Scientific and technical findings by NASA-sponsored contractors and grantees.

- CONFERENCE PUBLICATION. Collected papers from scientific and technical conferences, symposia, seminars, or other meetings sponsored or cosponsored by NASA.

- SPECIAL PUBLICATION. Scientific, technical, or historical information from NASA programs, projects, and mission, often concerned with subjects having substantial public interest.

- TECHNICAL TRANSLATION. English-language translations of foreign scientific and technical material pertinent to NASA's mission.

Specialized services that complement the STI Program Office's diverse offerings include creating custom thesauri, building customized databases, organizing and publishing research results…even providing videos.

For more information about the NASA STI Program Office, see the following:

- Access the NASA STI Program Home Page at ***http://www.sti.nasa.gov***

- E-mail your question via the Internet to help@sti.nasa.gov

- Fax your question to the NASA Access Help Desk at (301) 621-0134

- Telephone the NASA Access Help Desk at (301) 621-0390

- Write to:
  NASA Access Help Desk
  NASA Center for AeroSpace Information
  7121 Standard Drive
  Hanover, MD 21076-1320

NASA/TM-2003-212035

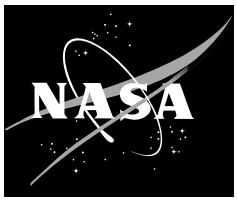

Ground-Effect Characteristics of the Tu-144 Supersonic Transport Airplane

Robert E. Curry
NASA Dryden Flight Research Center
Edwards, California

Lewis R. Owens
NASA Langley Research Center
Hampton, Virginia

National Aeronautics and
Space Administration

Dryden Flight Research Center
Edwards, California 93523-0273

October 2003

NOTICE

Use of trade names or names of manufacturers in this document does not constitute an official endorsement of such products or manufacturers, either expressed or implied, by the National Aeronautics and Space Administration.

Available from the following:

NASA Center for AeroSpace Information (CASI)
7121 Standard Drive
Hanover, MD 21076-1320
(301) 621-0390

National Technical Information Service (NTIS)
5285 Port Royal Road
Springfield, VA 22161-2171
(703) 487-4650

ABSTRACT

Ground-effect characteristics of the Tu-144 supersonic transport airplane have been obtained from flight and ground-based experiments to improve understanding of ground-effect phenomena for this class of vehicle. The flight test program included both dynamic measurements obtained during descending flight maneuvers and steady-state measurements obtained during level pass maneuvers over the runway. Both dynamic and steady-state wind-tunnel test data have been acquired for a simple planform model of the Tu-144 using a developmental model support system in the NASA Langley Research Center 14- by 22-ft Subsonic Wind Tunnel. Data from steady-state, full-configuration wind-tunnel tests of the Tu-144 are also presented. Results from the experimental methods are compared with results from simple computational methods (panel theory). A power law relationship has been shown to effectively fit the variation of lift with height above ground for all data sets. The combined data sets have been used to evaluate the test techniques and assess the sensitivity of ground effect to various parameters. Configuration details such as the fuselage, landing gear, canards, and engine flows have had little effect on the correlation between the various data sets. No distinct trend has been identified as a function of either flightpath angle or rate of descent.

NOMENCLATURE

a_x	acceleration in X body axis, *g*, positive forward
a_z	acceleration in Z body axis, *g*, positive down
b	span, ft
C_D	drag coefficient
C_L	lift coefficient
C_m	pitching moment coefficient about the reference center of gravity (40-percent *MAC*)
C_N	normal force coefficient, positive up
C_X	force coefficient in X body axis, positive forward
C_Z	force coefficient in Z body axis, positive down
DGE	dynamic ground effect
DGPS	differential global positioning system
h	height of the wing aerodynamic center above the ground, ft
HSCT	high-speed civil transport
I_x, I_y, I_z	moments of inertia about the X, Y, and Z axes, slugs-ft^2
k	constant
MAC	mean aerodynamic chord, ft
n1	stage one compressor rate of rotation for engine number 1, percent
NASA	National Aeronautics and Space Administration
OGE	out-of-ground effect

p	roll rate, rad/sec
q	pitch rate, rad/sec
$\bar{q}$	dynamic pressure, lb/ft^2
r	yaw rate, rad/sec
S	wing reference area, ft^2
T	thrust, lb
V	true airspeed, ft/sec
W	gross weight, lb
α	angle of attack, deg
γ	flightpath angle, positive for ascending flight, deg
δe	elevon position, deg
$\Delta C_{L_{GE}}$	incremental change in lift coefficient due to ground effect
θ	pitch attitude, deg

Subscripts

eff	flight conditions simulated through dynamic wind-tunnel testing
ref	adjusted to reference angle of attack and/or elevon position
uncorrected	dynamic wind-tunnel data prior to removal of inertial force components
α	partial derivative with respect to angle of attack
δe	partial derivative with respect to elevon position

INTRODUCTION

Aerodynamic ground effect is an important aspect in the design of large transport aircraft, because of the potential impact on takeoff and landing performance and flying qualities. Simulation, control system design, and performance predictions depend on accurate ground-effect models, which are usually obtained through proven analysis, wind-tunnel test techniques, and experience gained from similar configurations.

Slender wing configurations that have been proposed for an advanced high-speed civil transport (HSCT) aircraft (ref. 1) might exhibit ground-effect characteristics that are different from those of conventional subsonic transport aircraft. This issue was studied during initial supersonic transport aircraft development efforts in the 1960s (refs. 2, 3). Accepted aerodynamic theory indicates that ground effect at a particular nondimensional height above ground (*h/b*) will generally be more significant for comparatively lower-aspect ratio aircraft. Although ground effect has generally been approached as a steady-state situation, studies indicate that the rate of descent of an aircraft during landing might also induce “dynamic” aspects to the problem. Canards, aft-mounted underwing engines, and the presence of

vortex lift are other potential HSCT features that might influence ground-effect characteristics. The importance of these issues has emphasized the need for further study of ground effect and the reliability of test techniques for this new class of vehicle.

Ground-effect prediction has been a challenging problem for many reasons. Analytical methods have generally been based on steady-state flow superposition and engineering methods such as panel codes (refs. 4, 5). These methods have limited ability to incorporate configuration complexity such as high-lift system details and the modeling of engine exhaust flows. Wind-tunnel testing often has similar limitations and might invoke additional complications. A moving ground belt or other devices are often needed to remove the unrealistic boundary layer on the wind-tunnel ground plane simulation. Recent studies have attempted to also include dynamic effects (refs. 6, 7, 8). References 9–14 discuss ground-test methods that have been used to address the dynamic aspect of ground effect. Both analytical and wind-tunnel predictive methods have had few opportunities for validation.

Although flight tests might provide data to validate the performance of the predictive methods, these measurements are difficult to obtain. References 15–21 describe ground-effect measurements obtained for full-scale vehicles in flight and compare the measurements with predictive data. The parametric variations are limited when an aircraft is flown in close proximity to the ground. The vehicle must be kept close to trim, and sink rates must be controlled to avoid overstressing the landing gear. Flight measurements can be obtained in both steady-state (level flight over the ground) and dynamic (descending flightpath similar to landing) conditions; however, relating the ground-effect increments to a reliable out-of-ground effect (OGE) reference condition can be difficult. Because ground-effect increments are relatively small compared to other vehicle forces and moments, even small atmospheric disturbances can affect the quality of the flight data. Any wind across the runway has a boundary layer, or varying velocity profile, that will provide a systematic error in the ground-effect measurements.

As part of the NASA High-Speed Research program, the Tupolev Design Bureau modified a Tu-144 (Tupolev Aircraft Company, Moscow, Russia) supersonic transport aircraft for use as a flying test bed (ref. 22). The configuration and performance capability of the test bed, redesignated the Tu-144LL aircraft, are relevant to many HSCT issues, and seven experiments have been conducted (refs. 23, 24). One of these experiments was directed at the study of ground effect, which is the subject of this report.

The objective of the Tu-144 flight experiment was to measure the ground-effect characteristics through a range of flight conditions including steady-state and dynamic conditions. These results provide a database for evaluation of experimental and theoretical predictive methods.

Concurrent to the flight activity, a unique wind-tunnel model support system was developed to enable simulation of dynamic ground-effect conditions in the NASA Langley Research Center (Hampton, Virginia) 14- by 22-ft Subsonic Wind Tunnel. During initial evaluations of the developmental system, a simple planform model of the Tu-144 airplane was tested. Results from these pathfinder tests, conducted under both dynamic and steady-state conditions, were obtained for correlation with the flight data.

Steady-state, full-configuration wind-tunnel data for the Tu-144 in ground effect are also included in this study. These data were obtained during initial development of the Tu-144 airplane.

This report describes the flight and wind-tunnel test techniques and data analysis methods. Measurement uncertainties, issues, and limitations of the various methods are discussed. Ground-effect data from the experimental methods are compared with predictions from engineering methods (panel theory). A power law relationship for the ground-effect increments with respect to height above ground is presented and used to fit results from the various data sets for more detailed comparisons. The data sets are used to assess the significance of parameters (such as sink rate and configuration complexity) and to correlate with results from other aircraft configurations.

VEHICLE DESCRIPTION

A Tu-144 “D” model airplane, originally configured as a commercial supersonic passenger jet, was modified into a test bed for high-speed flight research (ref. 22). As part of the modification process, the original RD-36-51 engines were replaced with NK-321 engines (named for N.D. Kuznetsov, Samara Scientific and Technical Complex, Samara, Russia), and a research instrumentation system was installed. Flight tests were conducted at Zhukovsky Air Development Center (near Moscow, Russia) using the modified Tupolev Tu-144 supersonic transport airplane.

Figure 1 shows a three-view of the Tu-144 airplane, and table 1 summarizes essential physical properties. The vehicle has a double-delta-wing planform with an inboard leading-edge sweep angle of 76° and an outboard leading-edge sweep angle of 57°. The four engines are mounted in two separate pods below the wings. Pitch control is provided by symmetric deflection of the wing trailing-edge surfaces or elevons. Roll control is provided by differential deflection of the elevons.

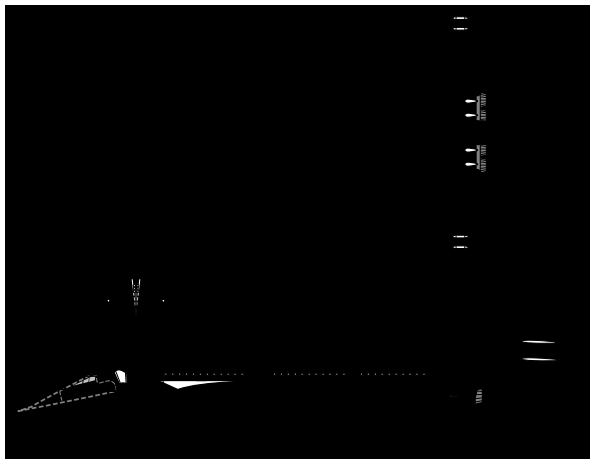

Figure 1. Three-view of the Tu-144 airplane.

Table 1. Physical properties of the Tu-144 airplane.

Reference area, ft^2	5457.8
Reference chord (*MAC*), ft	76
Reference span, ft	94.8
Reference center of gravity, percent *MAC*	40
Inboard leading-edge sweep, deg	76
Outboard leading-edge sweep, deg	57
Aspect ratio	1.65
Length overall, ft	220
Typical weight during test maneuvers, lb	265,000

During normal landings, the sharp nose section is canted downward (drooped) 17° to improve the pilot's field of view. For all maneuvers in this study, the nose was drooped and the landing gear were deployed. A highly cambered, unswept canard can be deployed just aft of the cockpit during normal landings. Maneuvers for this study were conducted with the canard retracted and deployed. Figure 2 shows a photograph of the Tu-144LL airplane in the normal landing configuration.

EC97-44203-03

Figure 2. Tu-144LL airplane in the normal landing configuration.

FLIGHT TESTING

This section discusses the flight testing of the Tu-144 airplane. The measurements, derived parameters, flight maneuvers, and data analysis are described in detail.

Measurements

The airplane was equipped with an extensive instrumentation system to support a variety of flight experiments including ground-effect research. A detailed description of this system is presented in reference 22. Data from a total of 1178 channels were acquired and encoded by a 12-bit pulse code modulation (PCM) system. The PCM stream was recorded on board with a digital tape recorder and personal computer. Primary measurements for the ground-effect data analysis were body axis linear accelerations, angular attitudes, angular rates, and control surface positions. Lateral and vertical accelerations were recorded at approximately 64 samples/sec, and the other flight dynamics parameters were recorded at 32 samples/sec.

An Ashtech Z-12 (Ashtech, Inc., Sunnyvale, California) carrier phase differential global positioning system (DGPS) satellite receiver was installed on board the Tu-144LL airplane. Data were obtained at a rate of 2 samples/sec, stored in the internal memory of the unit, and downloaded after each flight. These data were merged with data from a ground-based unit using the Ashtech Precise Differential GPS Navigation and Surveying (PNAV™) software (ref. 25). This software computes time and space position data and then derives other useful parameters such as flightpath angle and ground speed. The PNAV™ software also determines the root-mean-square uncertainty in the space position data. During the majority of the ground-effect testing, PNAV™ indicated uncertainties less than 0.3 ft.

Meteorological conditions in the vicinity of the runway were measured with conventional ground-based sensors. Windspeed and direction were recorded for each maneuver.

Derived Parameters

The height of the airplane above the ground was determined from the DGPS data and other onboard measurements. This derivation followed the approach described in reference 21 and is believed to offer the same level of uncertainty (less than ±0.5 ft). The DGPS directly measured the location in space of the onboard global positioning system antenna. The measurement of pitch attitude was used to determine the location of other points on the airplane, such as the reference center of gravity and the main landing gear, under the assumption that the airplane is a rigid body. The height above ground of the aerodynamic reference point was determined as the difference between the location of the reference point in space and an analytical model of the runway surface. The accuracy of this method was confirmed by checking the derived height values during times when the airplane was in contact with the runway. Details of these procedures and the runway model are presented in reference 22.

The measurement of pressure altitude was not used to determine height above ground, because the sensor calibration could be influenced by ground effect. For the same reason, the conventional onboard measurement of angle of attack (from a flow angle vane) was not used for analysis of the ground-effect maneuvers. Because tests were conducted only during low-windspeed conditions, angle of attack was derived from the DGPS flightpath angle and pitch attitude.

The pitch angle acceleration was determined by differentiating the pitch rate data. Linear accelerations at the reference center of gravity were determined by adjusting the accelerometer sensor values for radius of rotation and angular accelerations.

After each flight, the mass properties were derived from onboard fuel quantities recorded in flight. Thrust levels during the ground-effect maneuvers were estimated postflight using onboard recorded engine parameters.

Flight Maneuvers

Two types of flight maneuvers were used to collect ground-effect data. The first maneuver, called the constant-alpha approach, is based on a method developed in reference 18. Data were collected as the aircraft descended toward the runway in a "dynamic" ground-effect situation. In the second type of maneuver, called the level pass approach, data were obtained as the aircraft flew level passes over the runway in a "steady" ground-effect situation.

Prior to each constant-alpha maneuver, the pilot appropriately configured the airplane by extending the landing gear, canting the nose down 17°, and either deploying the canard or leaving it retracted. The airplane was then aligned in a descent toward the runway at a predetermined glide slope. After stabilizing at the desired flight conditions, the pilot attempted to hold the power constant and make minimal control surface inputs. As the airplane approached the runway and responded to ground effect, the pilot continued to hold the throttle constant and attempted to maintain a constant pitch attitude using longitudinal stick inputs. The maneuver was complete when either the airplane touched down or throttle adjustments were made.

Figure 3 shows a typical time history for a constant-alpha maneuver, including some of the maneuver setup and the data analysis time segment. The stage one compressor rate of rotation for engine number 1 (*n1*) is shown to indicate periods of constant thrust. The value for engine number 1 is representative of total thrust, because the four throttles were normally adjusted in unison. The interval that starts when thrust is held constant and ends with the onset of ground effect is referred to as the OGE period.

The constant-alpha approaches were attempted at a variety of OGE flight conditions; however, the range of flight conditions was constrained by the requirement to touchdown within acceptable vertical and horizontal speeds. Angle of attack was between 8.5° and 10.5° for all maneuvers. Weight changes required some variation in airspeed, but differences in canard position had a more significant impact on airspeed. Equivalent airspeed ranged from 170 to 181 knots with the canard extended and was approximately 200 knots with the canard retracted. Elevon position was also dependent on canard usage. The average elevon position was approximately 8° (trailing edge down) with the canard extended and –3° with the canard retracted. The pilot used the instrument landing system (ILS) glide slope indicator as an aid for setting up the initial glide slopes. Approaches were attempted at nominal flightpath angles between –2° and –3°. Figure 4 shows a summary of the initial OGE flight conditions for the constant-alpha maneuver.

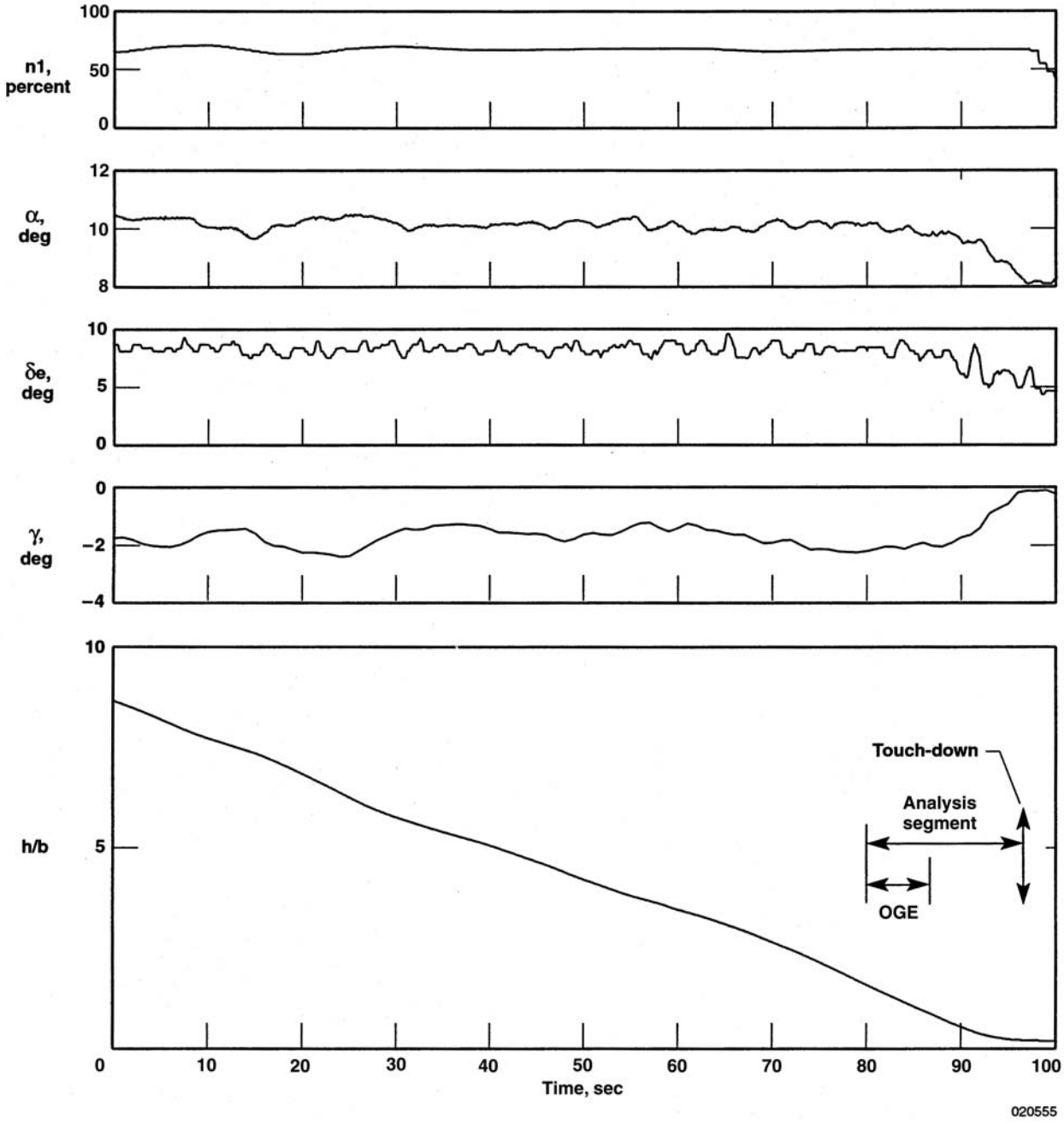

Figure 3. Typical time history for a constant-alpha maneuver.

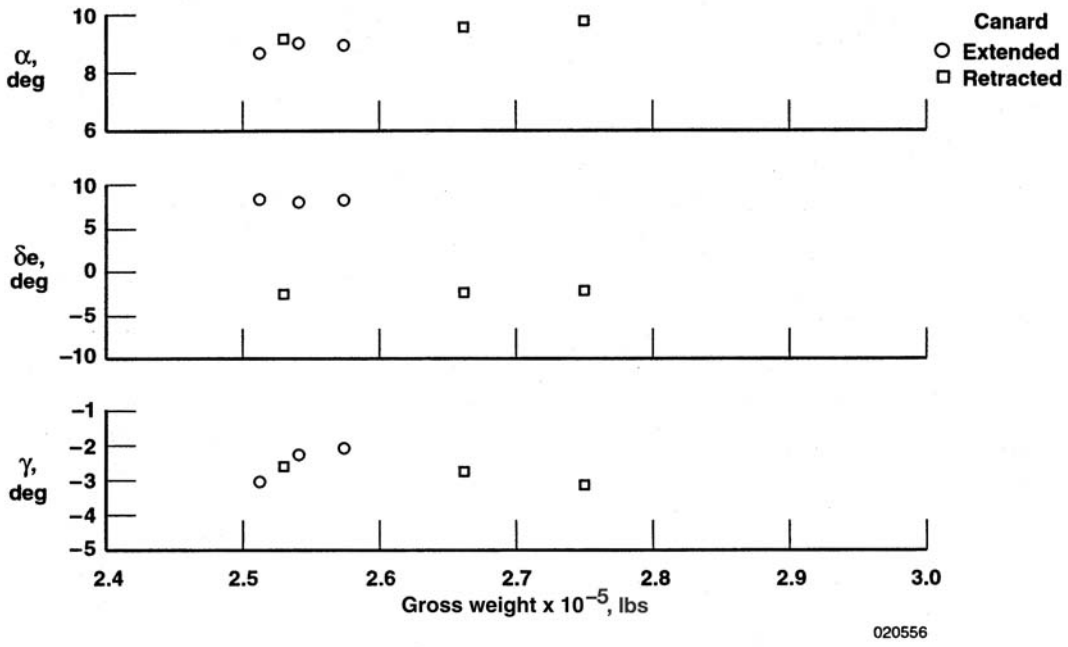

Figure 4. Out-of-ground effect flight conditions for the constant-alpha maneuver.

Maneuvers were rejected from further analysis if winds exceeded 5 knots in any direction, inconsistencies in the measurements were observed, or thrust was not held constant below 1.5 *h/b*. A total of 19 constant-alpha approaches were attempted, of which 6 were used for analysis.

For the level pass flight maneuver, the pilot approached the runway on a glide slope between –2° and –2.6° and then transitioned to level flight. These passes were conducted during low-windspeed conditions (less than 5 knots in any direction) with the canard extended and the nose canted downward. A total of 7 level pass flight maneuvers were conducted, from which 12 level segments were identified for analysis. To build confidence in the flight procedures, level passes were first conducted at 200 and 150 ft above ground before working downward to as low as 24 ft (wing height) above ground. During the level portions of the maneuver, the pilot attempted to minimize variations in thrust; however, throttle adjustments were generally necessary to adequately control the flightpath. Figure 5 shows a time history for a level pass maneuver. In this example, the airplane achieved two segments of level flight. The angle of attack and elevon positions during the second (and lowest) segment were approximately 5.2° and 5.9°, respectively. These conditions varied considerably from the OGE conditions for the constant-alpha maneuver (see figure 4).

The elevation of the runway varied considerably, and these maneuvers were actually flown parallel to the runway surface. This requirement, along with general safety concerns of conducting a nonstandard maneuver in close proximity to the ground, added considerable challenge to the level pass maneuver.

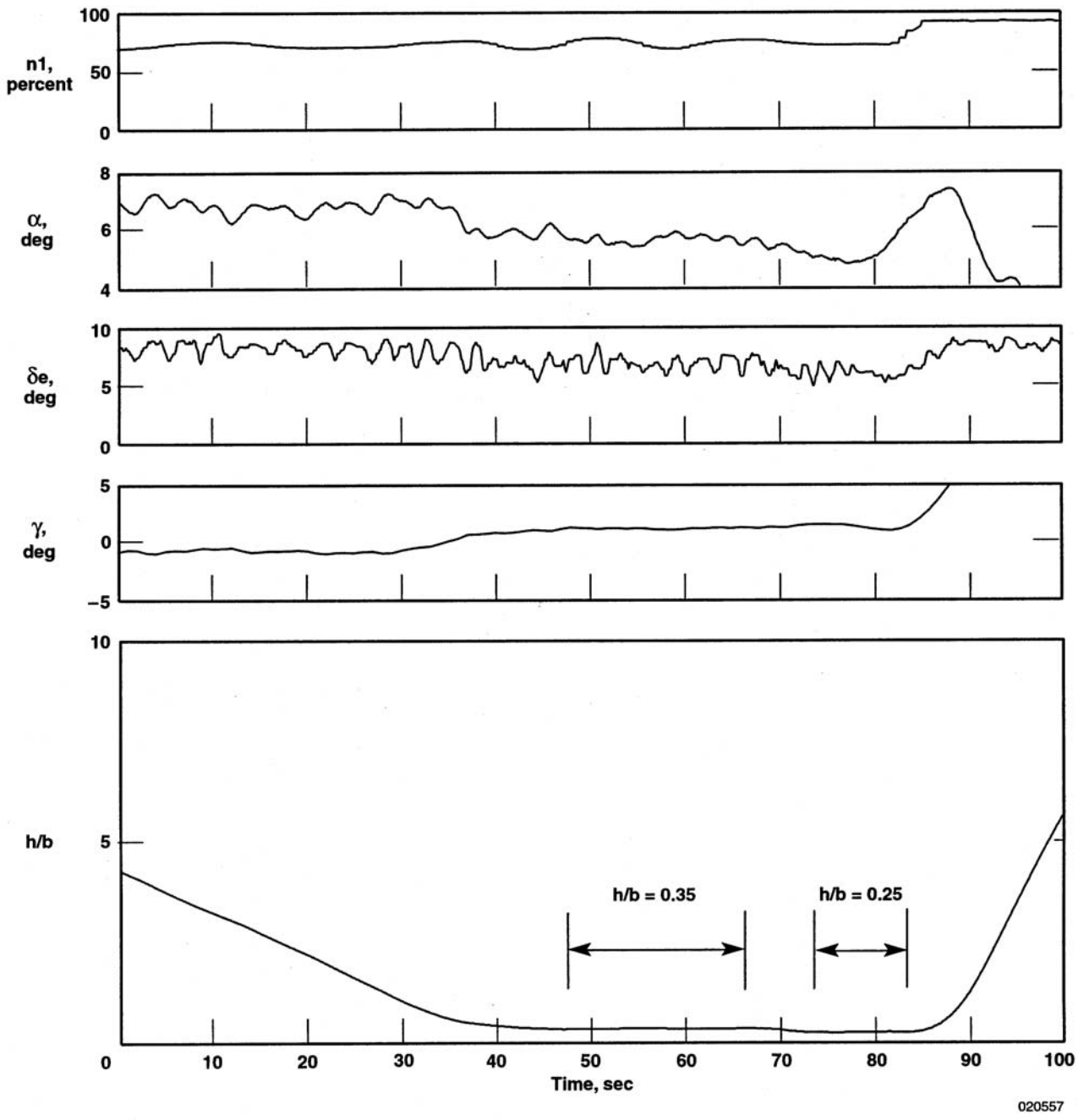

Figure 5. Typical time history for a level pass maneuver.

Data Analysis

Data analysis techniques for the constant-alpha approach were similar to the processes developed in reference 21. For each approach, a time interval was chosen during which the airplane was stabilized just before entering ground effect. Data from this OGE interval were averaged to determine OGE values for angle of attack, elevon position, flightpath angle, and thrust. The aerodynamic forces and moments acting on the airplane throughout the maneuver were then determined from the mass properties, thrust estimates, and measured body axis accelerations, using the following equations:

$$C_X = \frac{Wa_x - T}{S\bar{q}} \tag{1}$$

$$C_Z = \frac{Wa_z}{S\bar{q}} \tag{2}$$

$$C_m = \frac{I_y\dot{q} + (I_x - I_z)pr}{\bar{q}SMAC} \tag{3}$$

The pitching moments were calculated about the reference center of gravity. The forces were converted to stability axis lift and drag coefficients using the following equations:

$$C_L = -C_Z\cos(\alpha) + C_X\sin(\alpha) \tag{4}$$

$$C_D = -C_X\cos(\alpha) - C_Z\sin(\alpha) \tag{5}$$

Variations in elevon position and angle of attack occurred during each maneuver and generally increased as the airplane flew through ground effect. The effect of these variations had to be eliminated to determine the direct influence of ground effect. The average values of elevon position and angle of attack during the OGE portion of each maneuver were used as a reference from which the deviations could be measured. Aerodynamic derivatives were then used to extract the effects of trim changes that occurred during the maneuvers, as follows:

$$C_{L_{ref}} = C_L - C_{L_\alpha}(\alpha - \alpha_{OGE}) - C_{L_{\delta e}}(\delta e - \delta e_{OGE}) \tag{6}$$

$$C_{m_{ref}} = C_m - C_{m_\alpha}(\alpha - \alpha_{OGE}) - C_{m_{\delta e}}(\delta e - \delta e_{OGE}) \tag{7}$$

Because the value of C_m was close to zero during the maneuvers, changes in angle of attack and elevon position were the primary indications of ground effect. A table lookup function was used to correct the drag coefficient data,

$$C_{D_{ref}} = C_D - [C_D(\alpha, \delta e) - C_D(\alpha_{OGE}, \delta e_{OGE})] \tag{8}$$

These terms, $C_{L_{ref}}$, $C_{m_{ref}}$, and $C_{D_{ref}}$ are the aerodynamic coefficients of the airplane, referenced to the OGE trim conditions.

The aerodynamic derivatives used in equations 6–8, such as C_{L_α} and $C_{L_{\delta e}}$, and the drag function, were obtained from reference 23 and were assumed to be largely independent of ground effect. Because deviations from the reference conditions were typically small (< 3° in angle of attack, < 5° in elevon), this assumption was considered acceptable. Because the engine throttles were not adjusted during the constant-alpha approach, the incremental changes in the coefficients due to ground effect were not significantly affected by errors in the estimation of thrust.

Aerodynamic forces and moments for each level pass maneuver were determined in a similar manner. During each segment of level flight, the total aerodynamic and thrust forces acting on the airplane were determined from accelerometer and mass property data. Because throttle settings changed during the level pass maneuver, the postflight estimate of engine thrust was a critical input to this analysis. This variation in thrust was a significant disadvantage of the level pass maneuver compared to the constant-alpha approach in which thrust was held constant.

For comparisons with other data sets, the data for each level flight segment were corrected to a common reference trim condition (an angle of attack of 9° and an elevon position of 10°) using equations 6, 7, and 8. Because angle of attack changed considerably between the various level pass maneuvers, these corrections were more significant for the level pass approach data than for the constant-alpha approach data.

WIND TUNNEL TESTING

This section discusses the wind-tunnel testing of the Tu-144 airplane. The steady-state tests conducted by the Tupolev Design Bureau and both steady-state and dynamic tests conducted at NASA Langley are described in detail.

Tupolev Steady-State Testing

Wind-tunnel tests of the Tu-144 configuration in ground effect were conducted by the Tupolev Design Bureau during the initial development of the vehicle. A 4.8-percent scale model of the configuration was used, which included wing, body, vertical tail, nacelles, canards, and landing gear. Test conditions covered various heights above ground, flow angles, and control surface positions. The data are tabulated in reference 22. The wind-tunnel facility used for these tests did not incorporate a moving ground plane or other boundary-layer removal system. Reynolds number was 4×10^6 based on the model mean aerodynamic chord (*MAC*), 3.67 ft.

NASA Langley Steady-State and Dynamic Testing

In October 1997, tests were conducted in the NASA Langley 14- by 22-ft Subsonic Wind Tunnel (formerly the V/STOL Wind Tunnel and the 4×7 Meter Subsonic Tunnel). This atmospheric tunnel has

a contraction ratio of 9 to 1, is powered by an 8000-hp drive system, and has a large test section capable of a maximum speed of 318 ft/sec. Details of the test facility can be found in reference 26. Although the tunnel can be operated in either a closed or open test section configuration, the dynamic ground-effect tests were conducted with a closed-flow system. A boundary-layer removal system, located just upstream of the test section floor, was used.

A unique feature of the 14- by 22-ft Subsonic Wind Tunnel is that the model support hardware and floor of the test section are combined into removable units known as carts. A special cart, called the dynamic ground effect (DGE) cart, was developed to enable testing while a model is moved within the presence of ground effect. Figure 6 shows a diagram of the DGE cart. The large vertical support strut is hydraulically controlled to vary the model height above the cart (test section) floor. The strut has a hydraulic pitch drive that allows the model attitude to change during a dynamic plunge. The cart also has a yaw drive to simulate the effects of sideslip, although it was not used in this test.

A computer system controls the operation of the hydraulic mechanisms. The system executes a preprogrammed model trajectory in which a sequence of vertical speed and pitch attitudes is prescribed. The range of vertical travel extends from 89 in. to approximately 5 in. depending on the model and model pitch attitude. Model pitch limits range from –10° to +50°. Although the system is capable of a maximum vertical speed of 15 ft/sec, a maximum speed of 9 ft/sec was used in this test.

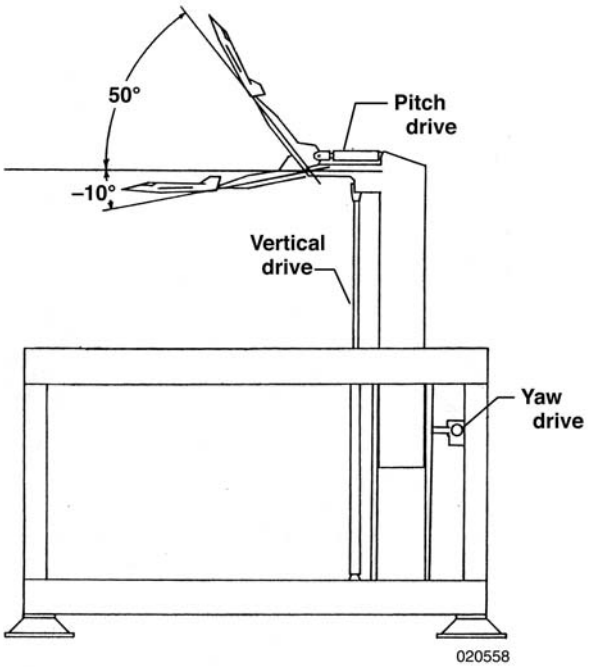

(a) Dynamic ground effect cart.

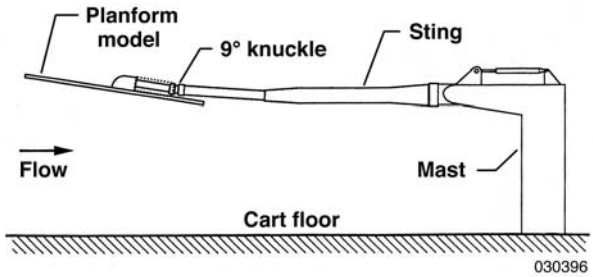

(b) Tu-144 planform model and sting configuration.

Figure 6. NASA Langley 14- by 22-ft Subsonic Wind Tunnel model support arrangement.

The October 1997 test was the first operation of the DGE cart, and the primary objective was to conduct a shakedown of the new system and related instrumentation. A detailed summary of this test is presented in reference 27.

One of several models tested during this developmental test was a planform representation of the Tu-144 airplane (fig. 7). The model has a wingspan of 47.1 in. and is approximately 4.1 percent the size of the flight vehicle. The model is constructed of sheet aluminum, covered with wood, and nominally contoured into a biconvex cross section with small radius leading edges. The elevon segments were set to 10° trailing edge down for these tests. The reference center of gravity for the model is consistent with the full-scale airplane (40 percent of the *MAC*).

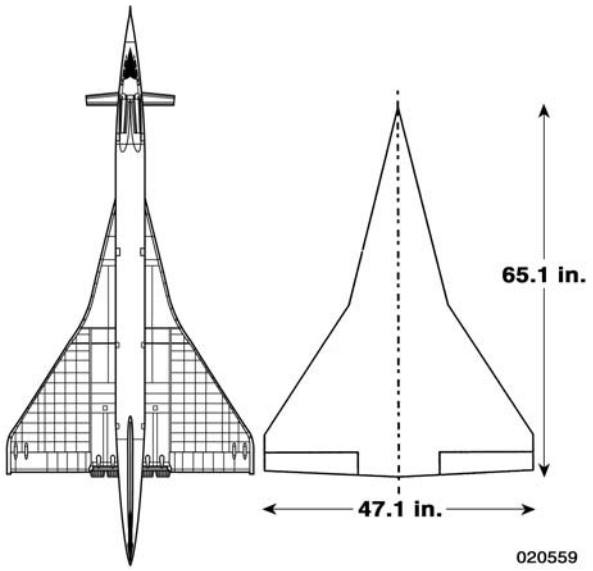

Figure 7. Comparison of the Tu-144 airplane and Tu-144 wing planform wind-tunnel model.

The model was attached to the sting through a balance block that was enclosed in a fairing and mounted to the upper surface of the model. The model and balance block weighed approximately 60 lb. A 9° knuckle was used to provide more angle-of-attack capability near the ground plane.

Wind-tunnel instrumentation included a force and moment balance, accelerometers, and an optical tracking system. Six model accelerometers were used in combination to provide three linear and three angular accelerations of the model reference center. These data were used to remove inertial effects from the dynamic test data (discussed in the last paragraph of this section). Optical measurements were used to determine the height of the model relative to the tunnel floor at two different model locations. These data were used to define model height above the floor (ground plane), vertical speed, and pitch attitude relative to the tunnel axis system. Vertical speed data from differentiation of the position measurements were confirmed by integration of sting-mounted accelerometer data.

All data in this study were obtained at a tunnel velocity of 267 ft/sec. Vector analysis was used to determine the effective model airspeed, angle of attack, and flightpath angle from the tunnel speed and optical tracking system data, as shown:

$$V_{eff} = \sqrt{267^2 + \dot{h}^2} \tag{9}$$

$$\gamma_{eff} = \sin^{-1}\left(\frac{\dot{h}}{V_{eff}}\right) \tag{10}$$

$$\alpha_{eff} = \theta - \gamma_{eff} \tag{11}$$

The wind-tunnel testing included a series of steady-state runs through a sweep of angles of attack. During these runs, the wing aerodynamic reference point was placed near the center of the tunnel at a height of 6 ft (h/b = 1.53). This position was assumed to be essentially OGE. Data from these runs were analyzed using conventional methods. Tares were determined from measurements taken during wind-off conditions.

A second series of steady-state runs was conducted with the model positioned at lower heights above the ground plane (h/b = 1.019, 0.509, 0.382, and 0.256) and at angles of attack of 7°, 9°, and 11°. These runs provided steady-state ground-effect data for the wing planform model.

Prior to dynamic testing, the model was rapped with a rubber hammer to excite the natural vibration modes of the combined model and sting support system. These vibration data, taken with no airflow, were used to relate the model accelerations to inertial forces sensed at the balance.

The model support system was then used to plunge the model vertically toward the ground plane. The effective flightpath angles for these runs ranged from approximately –0.2° to –2.5°. The model pitch attitude was set as a function of vertical velocity for each run so that all runs were conducted at the same effective angle of attack (approximately 9.55°). All derived lift coefficients, therefore, were referenced to this angle of attack using the OGE lift data for the wing planform.

Figure 8 shows typical time histories for two of the dynamic plunge tests. Data acquired from a low vertical speed run (2.2 ft/sec) (fig. 8(a)) shows a brief acceleration interval followed by a significant period of constant-speed conditions. Large oscillations in the model speed and measured normal force during startup were the result of inertial forces induced by the rapid acceleration of the model and subsequent “ringing” of the model and sting system. In this example, the inertial ringing ceased early in the run. An attempt was made to remove the inertial forces from the measurements using the relationship between accelerometer data and normal force data obtained during the wind-off vibrations. As shown in figure 8(a), this correction did not significantly improve the data during the initial acceleration but made a small improvement for heights between 0.3 and 1.3 h/b. Figure 8(b) shows a time history for a higher speed plunge (6.7 ft/sec). Because of the higher speed, most of the trajectory was affected by the acceleration and deceleration phases. The acceleration-based correction for inertial forces in C_N significantly improved the results, although it did not completely remove the inertial effects in the data. A test interval in which averaged conditions were constant was selected for these runs, although oscillations persisted throughout the run. Further details regarding the inertial correction process are provided in reference 27.

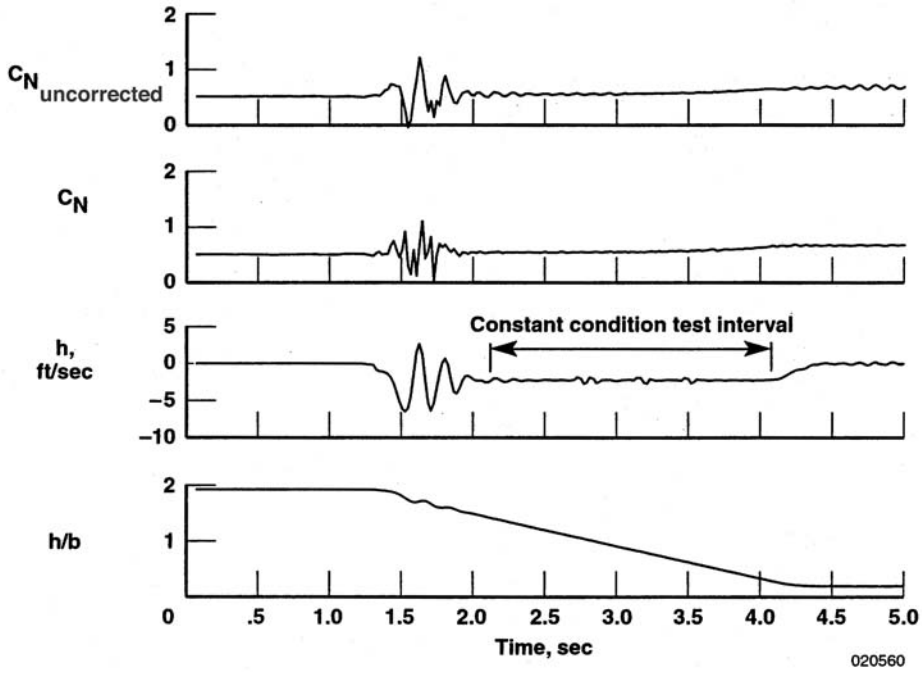

(a) Vertical speed approximately 2.2 ft/sec.

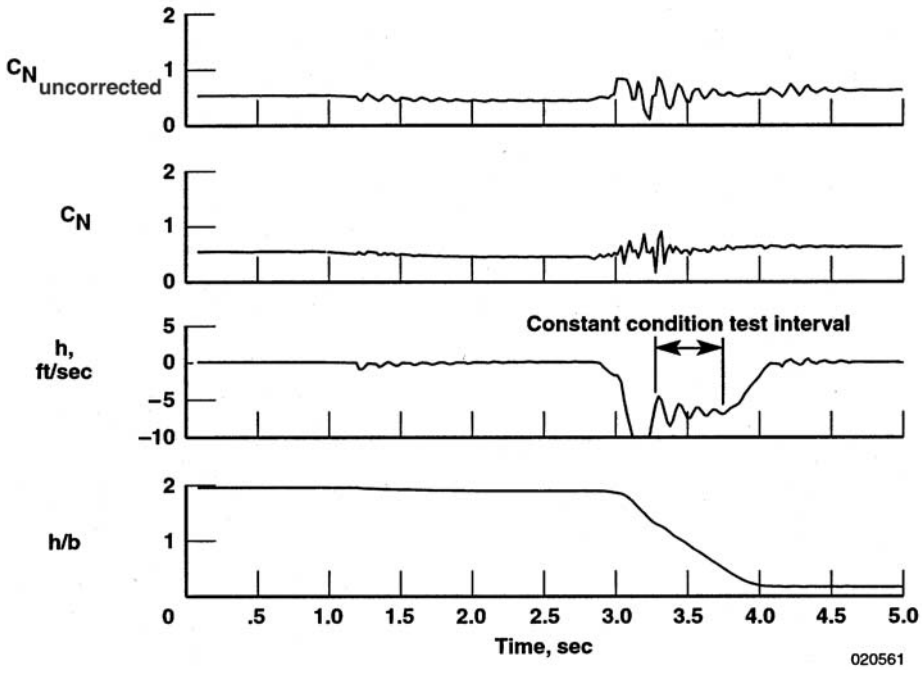

(b) Vertical speed approximately 6.7 ft/sec.

Figure 8. Time histories for dynamic plunge tests in the NASA Langley 14- by 22-ft Subsonic Wind Tunnel.

ANALYTICAL RESULTS

A constant-pressure, potential-flow, panel method (ref. 5) was used to predict ground-effect characteristics of the Tu-144 wing. A simple wing planform model was generated and used to determine the OGE characteristics without the presence of a ground plane. No attempt was made to include the correct camber distribution or trailing-edge flap deflections in the model. The presence of the ground was then simulated by including an image of the isolated wing. The plane of symmetry between the two wings served as an effective ground plane. The aerodynamic forces in ground effect were determined by integrating the panel pressures on the actual wing.

The resulting aerodynamic forces were then resolved into a lift component and drag component. The drag calculation includes only the lift-related or induced component of drag, because the panel code does not include viscous forces. In a similar manner, pitching moment about the aerodynamic reference point was determined by integrating the contributions from each panel.

Figure 9 shows results from the panel method. Because of the linear nature of potential flow theory, the computed forces were normalized by the corresponding OGE value. The normalized effects on lift and induced drag are identical.

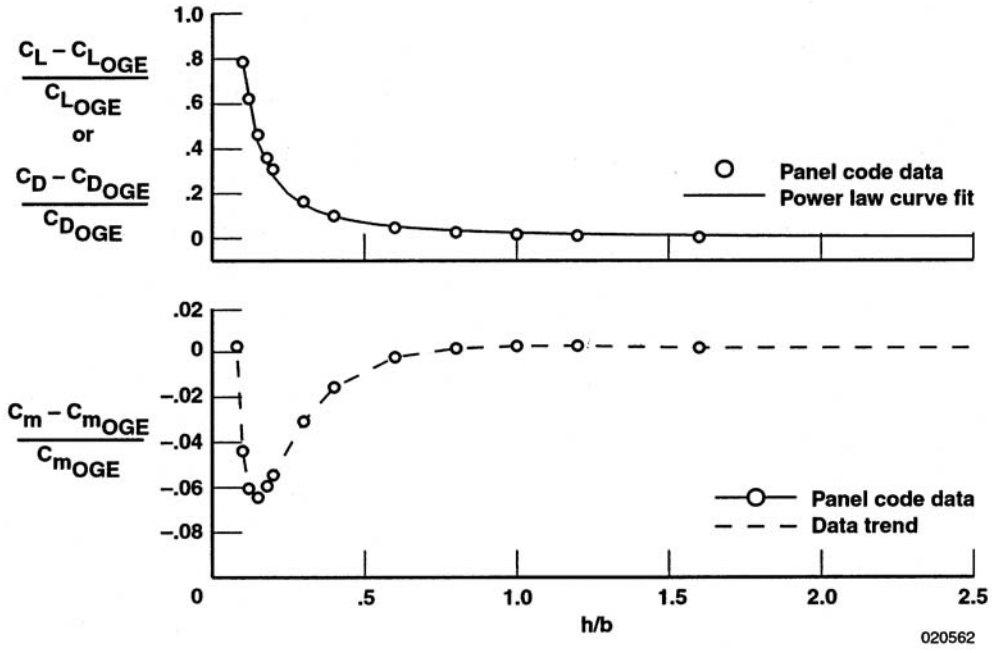

Figure 9. Panel code normalized ground-effect predictions.

As suggested by analysis in reference 28, the variation of normalized ground-effect increments with nondimensional height above ground was found to fit a –1.5 power law relationship as shown:

$$\frac{\Delta C_{L_{GE}}}{C_{L_{OGE}}} = \mathrm{k}\left(\frac{h}{b}\right)^{-1.5} \tag{12}$$

A least-squares curve fit method was used to determine the coefficient, k, for the panel code lift and drag data. As shown in figure 9, the resulting curve effectively represents the panel code data. As a result, the –1.5 power law relationship was also used in the interpretation of the experimental force data acquired in this study. Pitching moment variations with height above ground are more complicated and do not fit the power law relationship.

RESULTS AND DISCUSSION

Table 2 presents a summary of the nominal test configurations and conditions that are discussed in this report.

Table 2. Summary of nominal test configurations and conditions.

Data Set	α, deg	δe, deg	γ, deg
Flight (complete vehicle)			
Dynamic (constant-alpha maneuver)			
Canard extended	9	8	–2.1 to –3.0
Canard retracted	9.5	–2.5	–2.6 to –3.1
Steady-state (level pass maneuver)	varies	varies	0
Tupelov Wind Tunnel (complete vehicle)			
Steady-state	6,10,15	0,5,10	0
NASA Langley Wind Tunnel (wing planform)			
Dynamic	9.5	10	–.24 to –2.15
Steady-state	7,9,11	10	0
Analytical Data (wing planform)			
Steady-state	varies	0	0

Lift, drag, and pitching moment data from six constant-alpha maneuvers are shown as a function of nondimensional height above ground (*h/b*) (fig. 10). As previously discussed, the data are shown in coefficient form, referenced to the angle of attack and elevon position of the airplane immediately before entering ground effect. The coefficient data are unaffected by proximity to the ground at heights above one span (*h/b* = 1). Below this level, the influence of the ground on each coefficient is increasingly evident in all maneuvers.

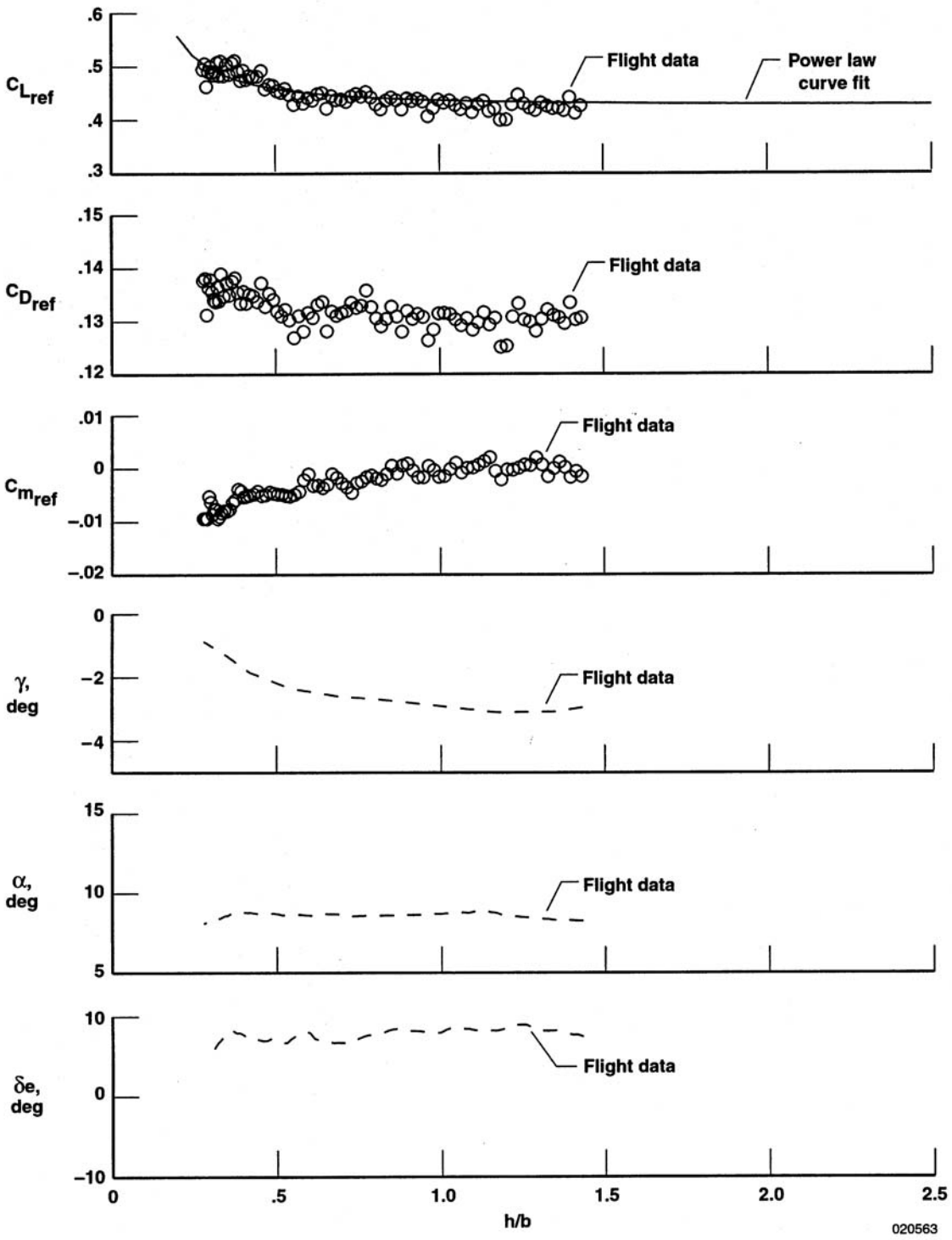

(a) Flight 4.

Figure 10. Constant-alpha maneuver data.

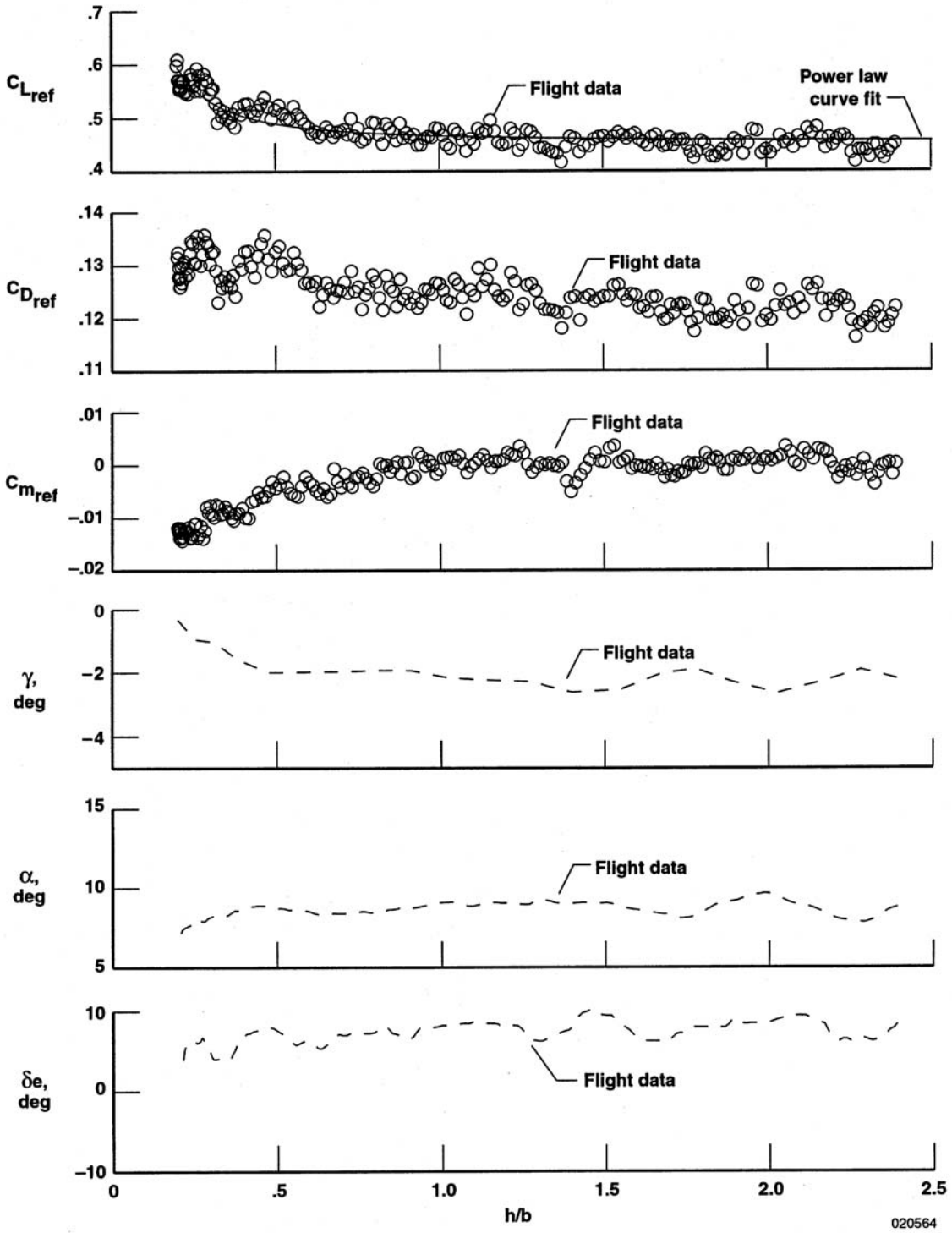

(b) Flight 5.

Figure 10. Continued.

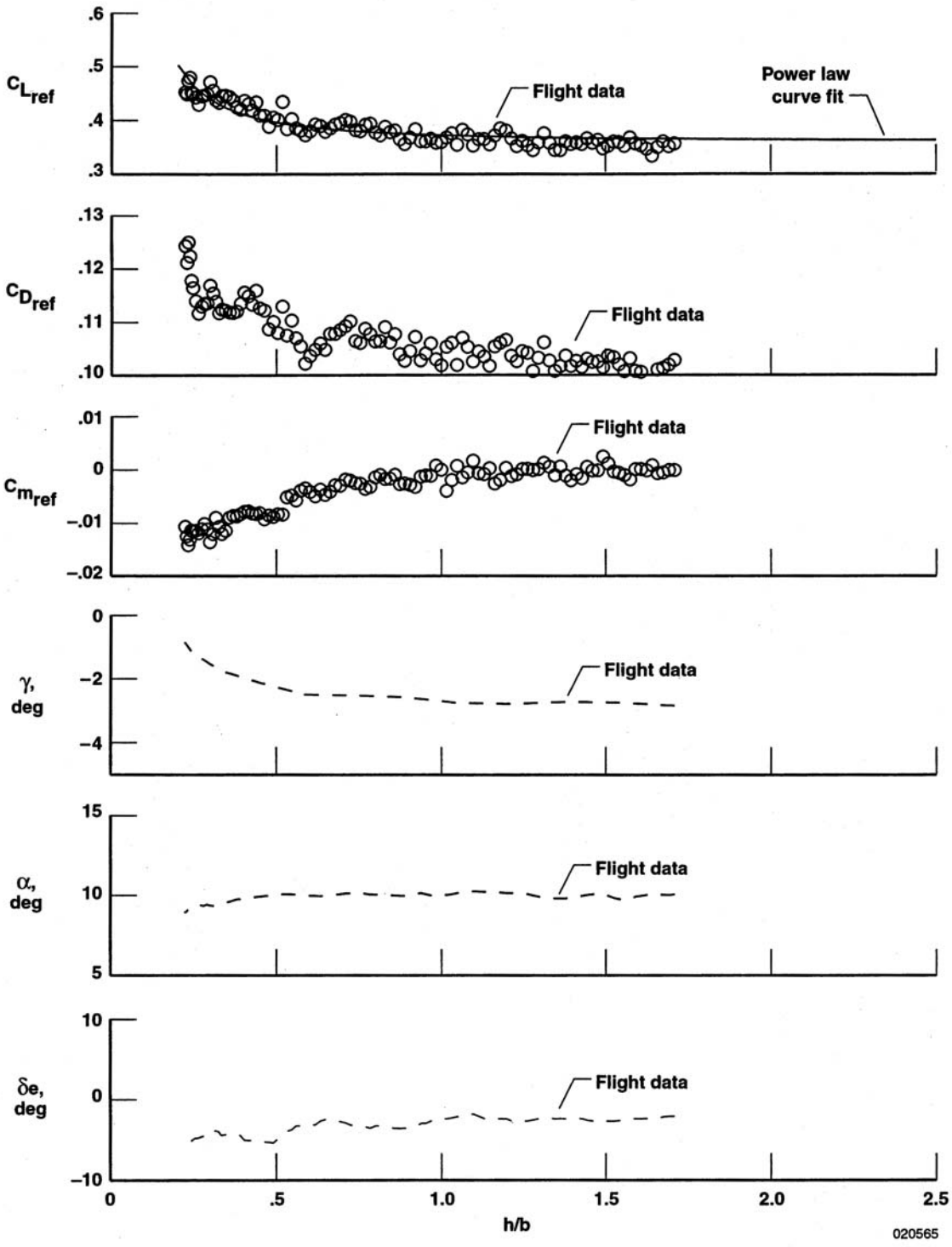

(c) Flight 12.

Figure 10. Continued.

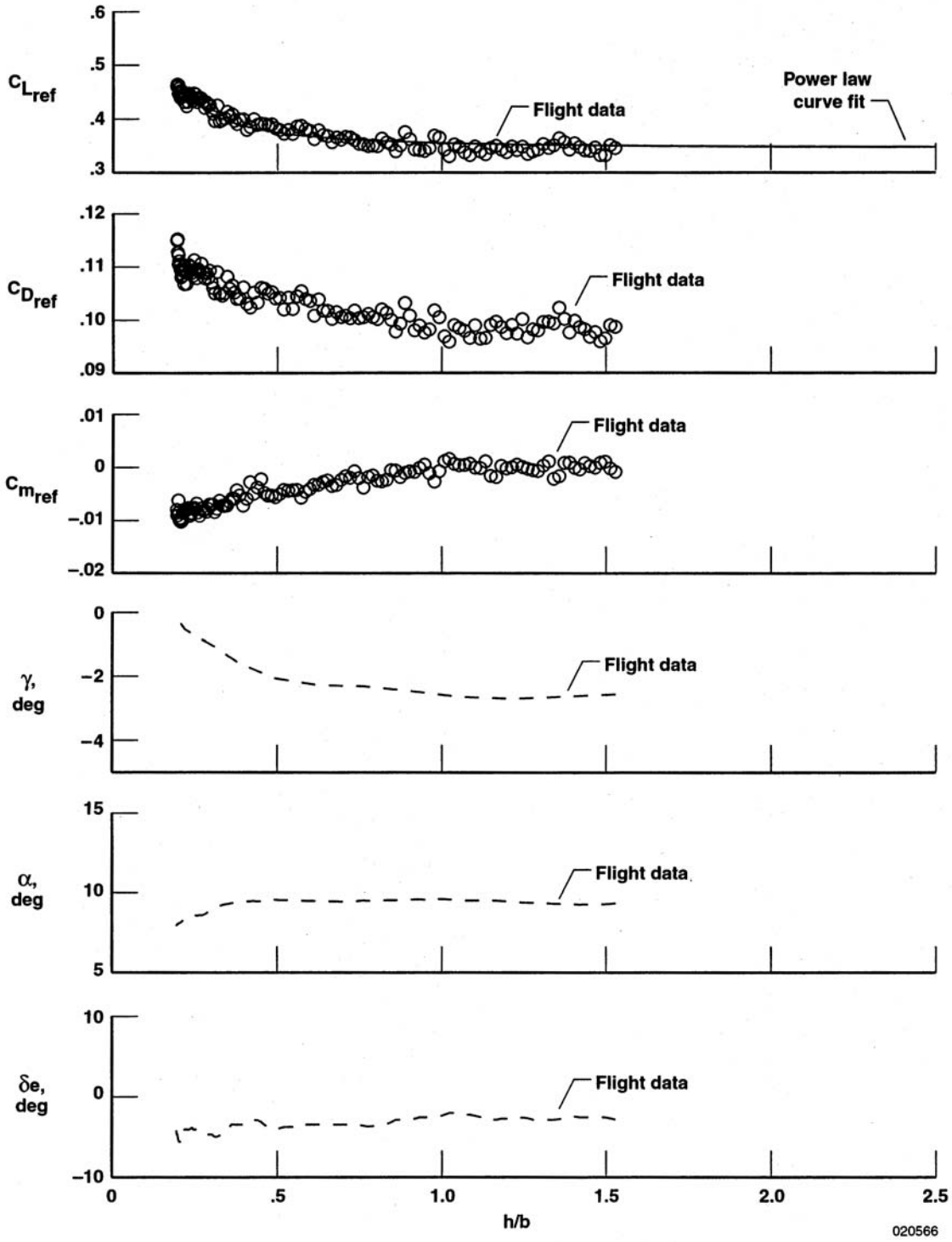

(d) Flight 13.

Figure 10. Continued.

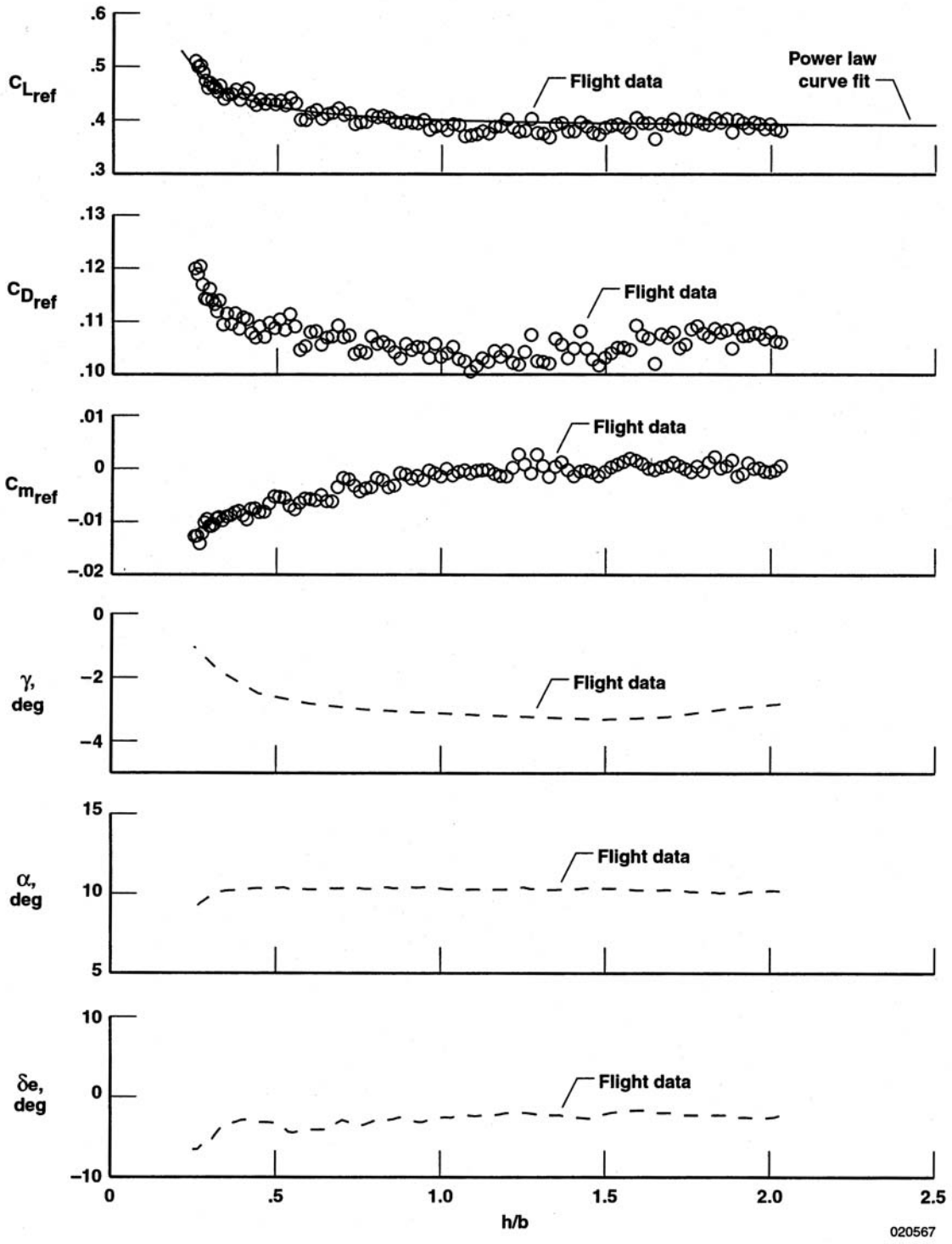

(e) Flight 14.

Figure 10. Continued.

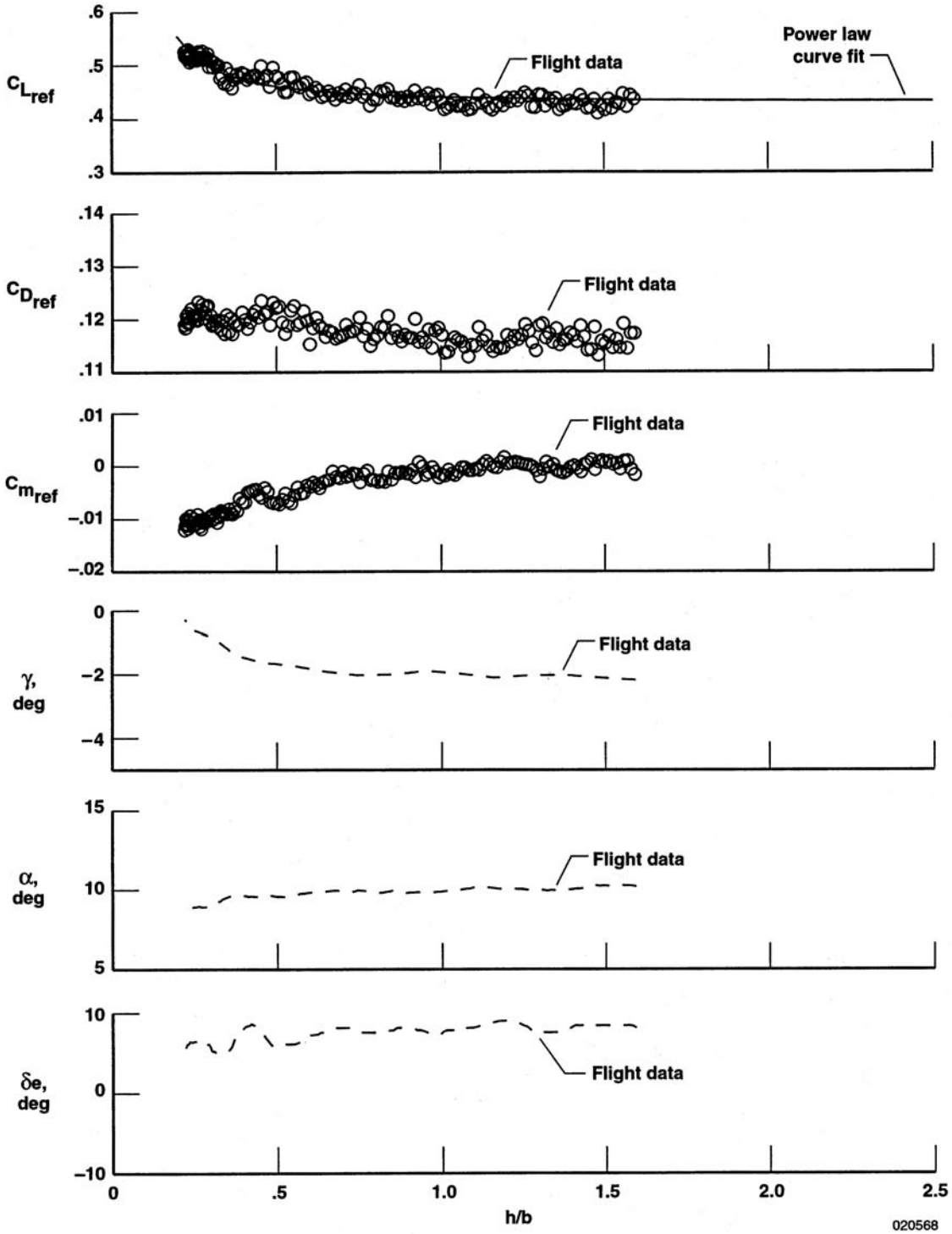

(f) Flight 16.

Figure 10. Concluded.

Figure 10 also shows flightpath angle, angle of attack, and elevon position for each maneuver. Although these parameters were relatively constant before entering ground effect, the flightpath angle, γ, became less negative as the airplane approached the runway. This effect occurred while angle of attack remained constant or even decreased in some cases. This natural flaring of the flightpath is a distinct indication of increased lift due to ground effect. Although the constant-alpha maneuvers provided data in a dynamic ground-effect situation ($\gamma \neq 0$), the rate of descent was not constant.

Because the pilot attempted to maintain a stabilized glide slope before entering ground effect, variations in the data obtained during the OGE portion of each maneuver ($h/b > 1$) indicate the quality of the force and moment measurements. The variations from the mean were calculated during the OGE time intervals, and standard deviations in the lift, drag, and pitching moment coefficients were found to be approximately 0.02, 0.003, and 0.002, respectively. These uncertainties are primarily attributed to atmospheric disturbances, sensor noise, and residual oscillatory dynamics (not included in the force and moment calculations).

A least-squares method was used to fit the lift data to a –1.5 power law relationship with the height above ground, as discussed earlier. Although the resulting curves (also shown in figure 10) match the general trend of the flight data, the fit is not as good as that of the analytical data in figure 9. Despite this case, the power law curve fit process is believed to provide a useful method for extracting data at specific altitudes for correlation with other data sets.

The consistency of the lift and pitching moment data is better than that of the drag data, which is expected, because the absolute magnitude of the drag increment caused by ground effect is much smaller than the force increment in the lift axis. Similar results were observed in previous ground-effect flight test studies (refs. 20, 21).

Figure 11 shows lift and pitching moment coefficients from the level pass maneuvers. As previously discussed, the data have been adjusted to a common set of reference conditions (an angle of attack of 9° and an elevon position of 10°). Because thrust levels varied with each level pass maneuver, drag measurements were not reliable.

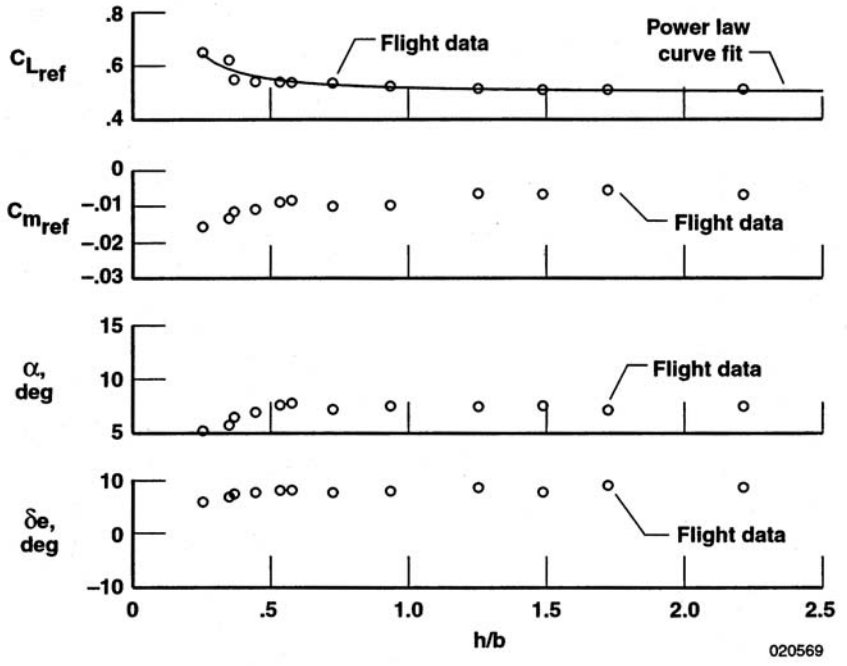

Figure 11. Level pass maneuver data.

Compared to the constant-alpha maneuver, the level pass maneuver has several deficiencies. First, seven level pass maneuvers were required to obtain the data in figure 11, whereas each constant-alpha maneuver provided an equivalent set of data. The level pass technique is clearly less efficient in terms of flight test operations. Second, the lift and pitching moment data from the level pass maneuvers are less consistent than the data from the constant-alpha approaches. Whereas the constant-alpha maneuver data analysis extracts ground effect from an incremental change in the forces and moments that occur during the same maneuver, the level pass maneuver data analysis requires correlation of data from multiple maneuvers. This lack of reference is believed to have introduced errors that were not completely accounted for in the analysis process and is a fundamental disadvantage of the level pass test technique.

Figure 12 shows full-configuration, steady-state lift coefficient results at three elevon settings, each at three angles of attack, from the Tupolev wind-tunnel test. When each set of ground-effect increments are divided by the corresponding OGE lift coefficient, the normalized data sets collapse into a common trend. Each set of data fits the –1.5 power law relationship reasonably well.

Similar results were found in the lift coefficient data from the wing planform model tests, which were conducted in the NASA Langley wind tunnel under steady-state conditions (fig. 13). As shown, the consistency of the wing planform data is very good.

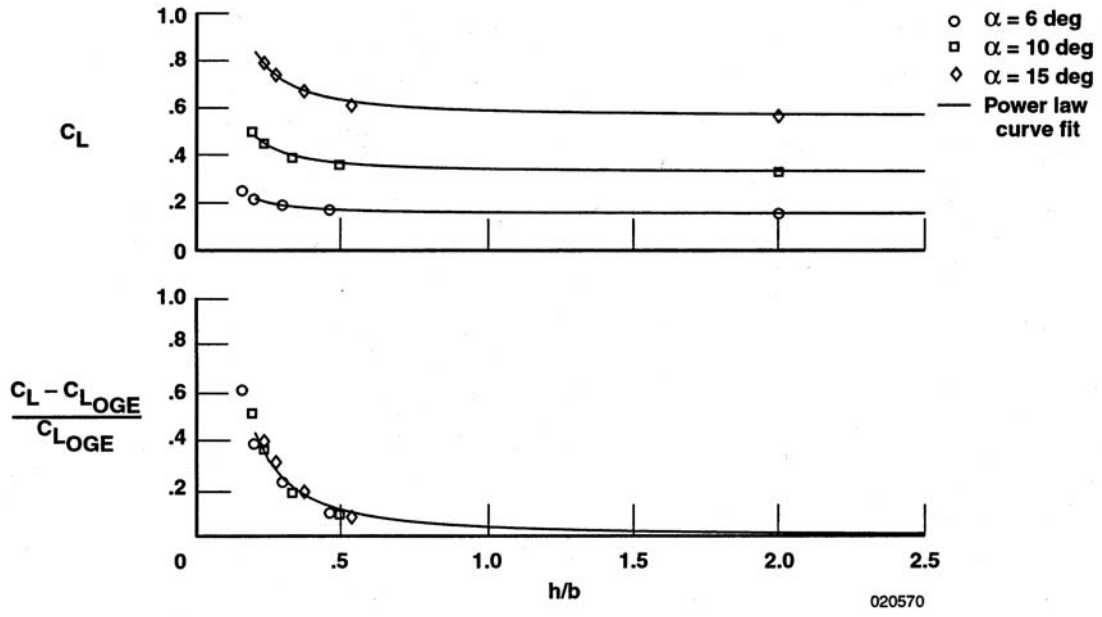

(a) $\delta e = 0°$.

Figure 12. Full-configuration, steady-state wind-tunnel test data.

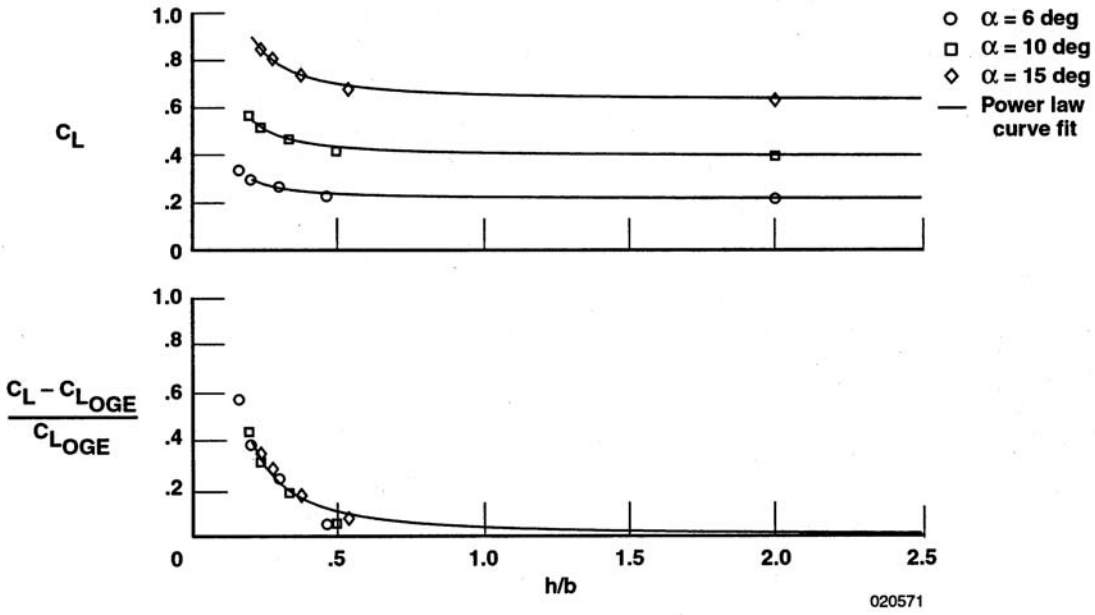

(b) $\delta e = 5°$.

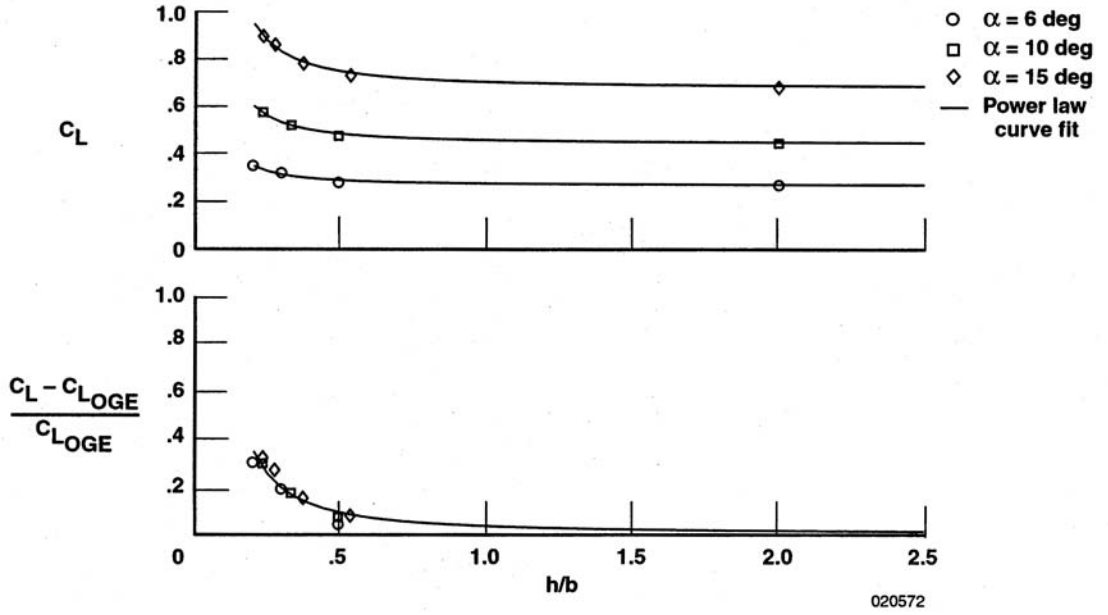

(c) $\delta e = 10°$.

Figure 12. Concluded.

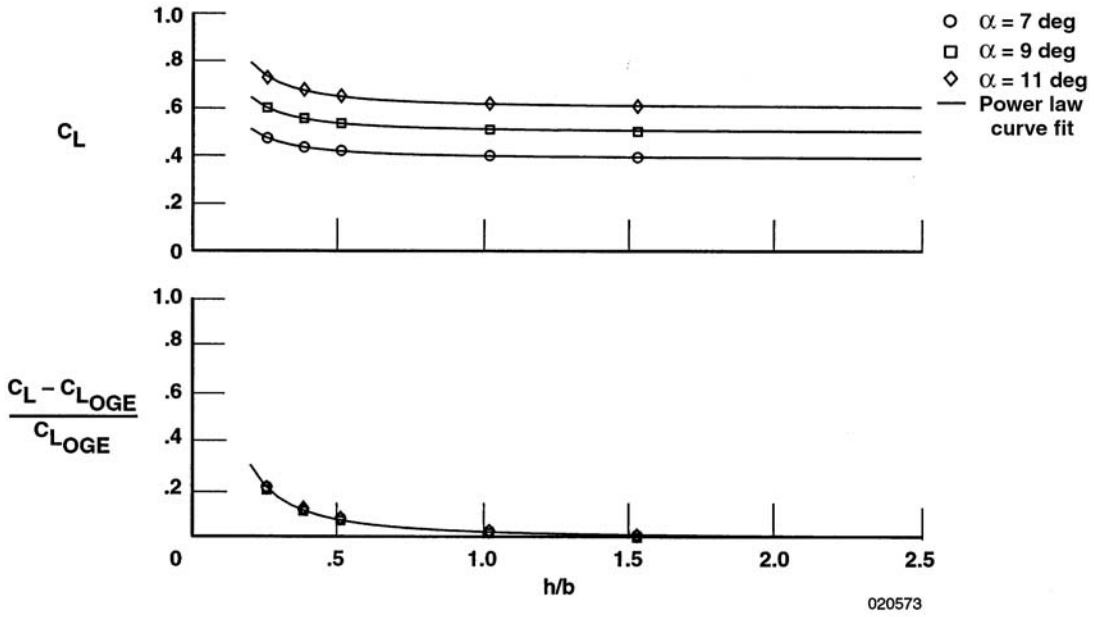

Figure 13. Steady-state wind-tunnel test data of the wing planform model, $\delta e = 10°$.

Figure 14 shows lift coefficient data, effective flightpath angle, and angle of attack from dynamic wind-tunnel testing of the wing planform model. Considerable scatter is present in both the trajectory data and the lift coefficient data acquired at the beginning of each run ($h/b \approx 1.5$). The scatter was caused by inertial forces and motions from the acceleration of the model. After this startup transient, the angle of attack and flightpath angle were constant at the lower flightpath angles for the remainder of the two runs (figs. 14(a) and 14(b)). For runs at higher flightpath angles (higher vertical velocities), the angle of attack and flightpath angle decreased as the model decelerated at the end of the run. As previously discussed, the effective angle of attack during the constant-rate portion of each run was 9.55°, and all lift coefficient data shown for this test have been referenced to an angle of attack of 9.55° for consistency.

To test the wind-tunnel measurements and analysis techniques, data derived from the dynamic runs were compared with steady-state measurements for the same model. For the dynamic tests, the planform model had a lift coefficient of 0.532 during the initial descent (above ground effect) at an effective angle of attack of 9.55°. These data compare well with the steady-state data.

For runs that simulated flightpath angles steeper than –1° (figs. 14(d), 14(e), and 14(f)), the entire trajectories were at varying conditions. Although an increase in the lift coefficient caused by ground proximity is evident in every case, the quality of the data degraded to an unusable level as runs were conducted at the higher descent rates.

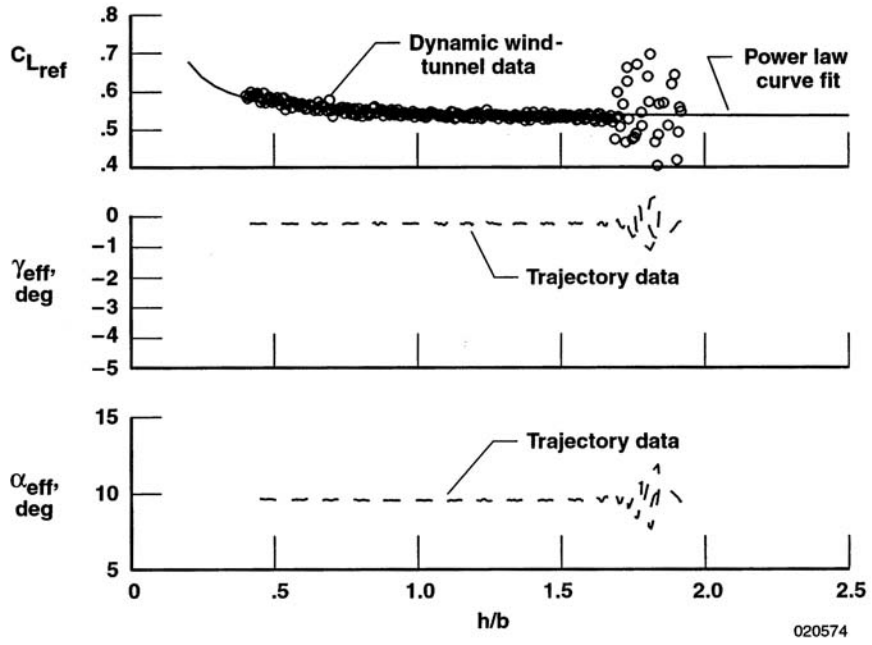

(a) Nominal flightpath angle = –.24°.

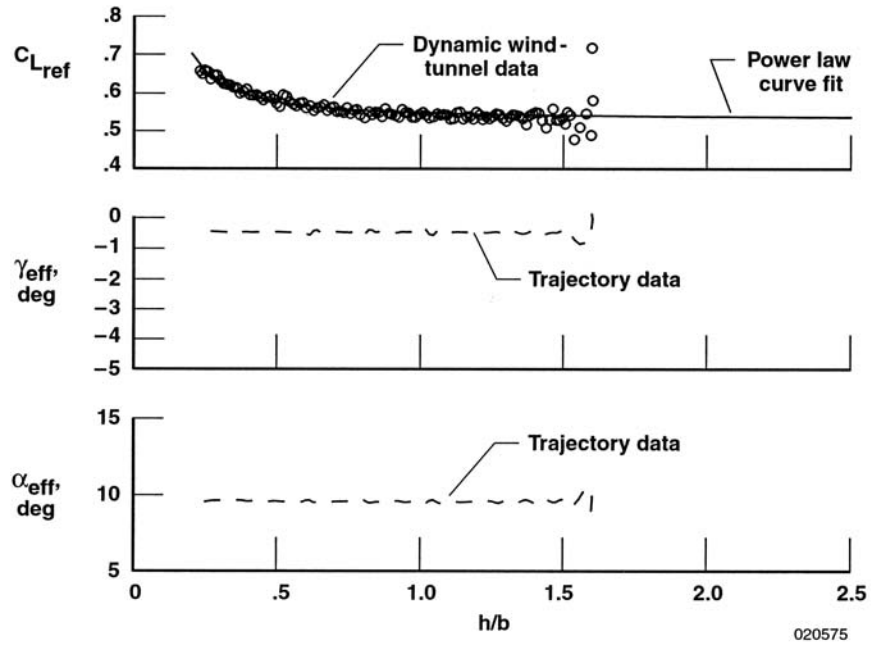

(b) Nominal flightpath angle = –.48°.

Figure 14. Dynamic wind-tunnel test data of the wing planform model, δe=10°.

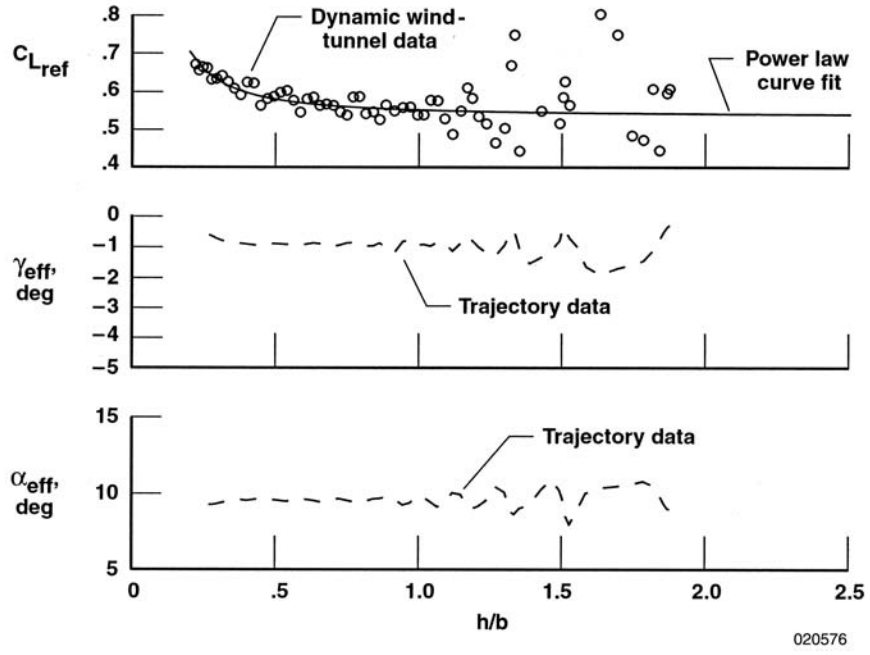

(c) Nominal flightpath angle = –.98°.

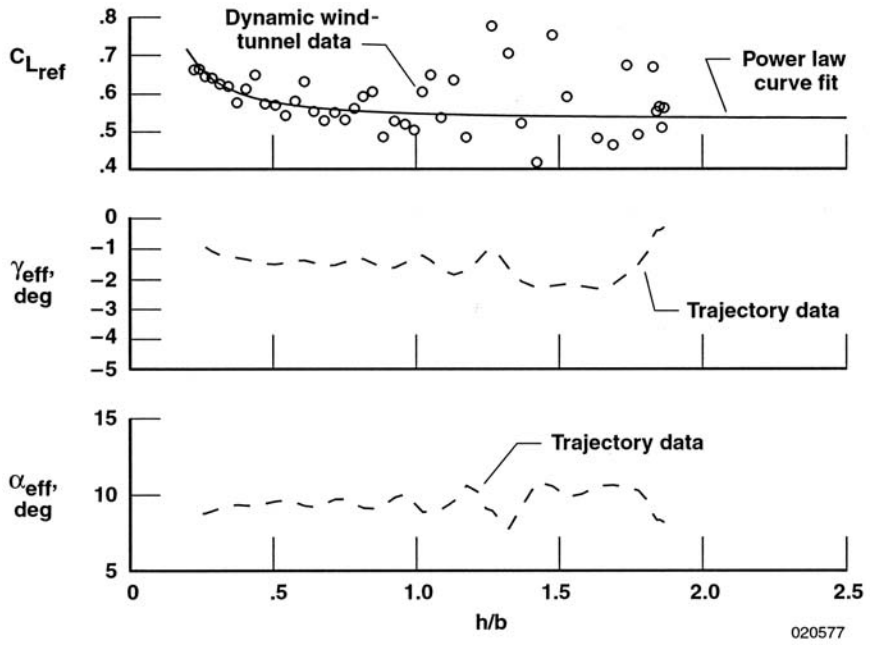

(d) Nominal flightpath angle = –1.49°.

Figure 14. Continued.

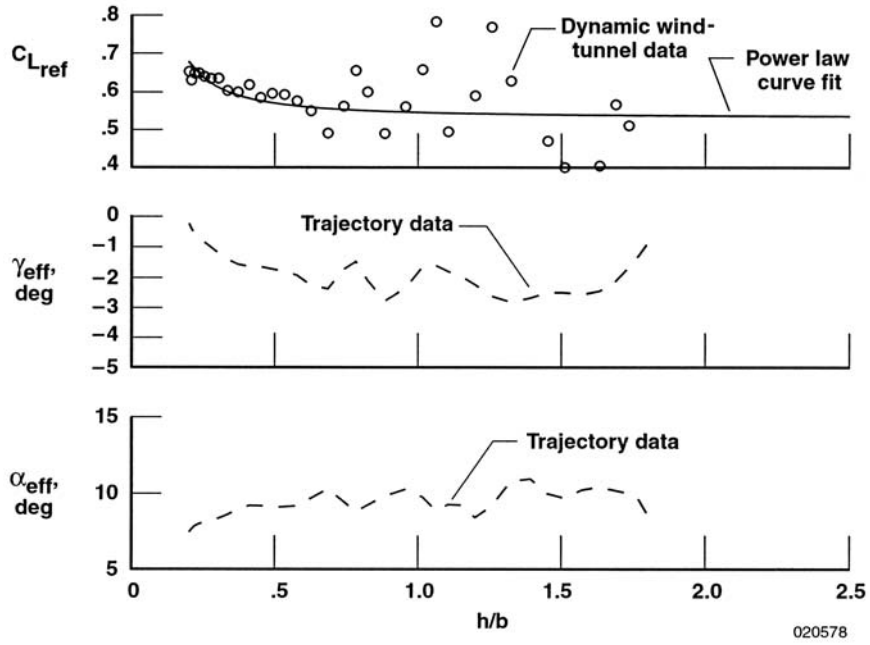

(e) Nominal flightpath angle = –2.17°.

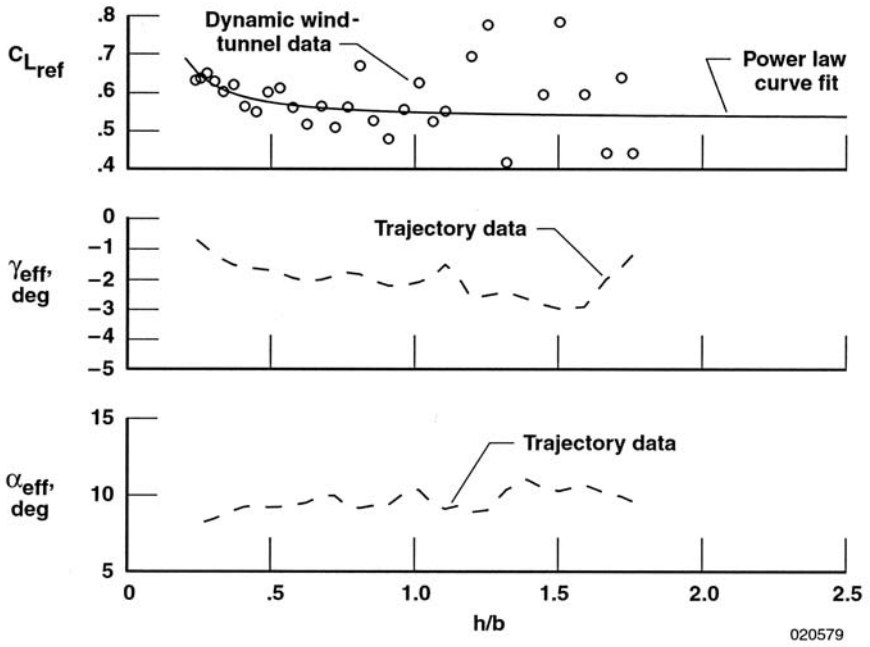

(f) Nominal flightpath angle = –2.15 °.

Figure 14. Concluded.

To be able to compare the results from the various data sets discussed in this report, the lift increments caused by ground effect were normalized to the corresponding OGE conditions. The power law curve fit was applied to each data set and used to determine a normalized lift coefficient increment at a common height above ground (h/b = 0.3 was chosen, because it fell within the range of all the test techniques). Figure 15 shows the resulting data as functions of flightpath angle, angle of attack, and elevon position.

Figure 15(a) shows no distinct variation in normalized lift coefficient increments as a function of flightpath angle, although the level pass value is larger than the other data. The normalized lift coefficients from dynamic flight testing ($\gamma < 0$) are equivalent to the full-configuration, steady-state wind-tunnel data. Comparisons of the planform data sets in figure 15(a) also indicate no apparent trend resulting from a dynamic rate of descent (flightpath angle). With the exception of the level pass data, any relationship between lift coefficient ground effect and flightpath angle for this configuration is within the measurement accuracy of these methods.

This finding conflicts with results from other studies (refs. 6–14) that have identified differences in ground effect related to rate of descent. In some cases, particularly for highly swept configurations, ratios of steady-state to dynamic ground-effect coefficients as large as 2 have been reported. Such a large ratio is not evident in the Tu-144 data sets.

Figure 15(a) also indicates that ground effect for this vehicle is not a strong function of other parameters. For example, the full-configuration wind-tunnel test data, which had no engine exhaust flow simulation and were obtained at low Reynolds numbers, compare reasonably well to the full-scale flight test data. Furthermore, results from the simple, uncambered wing planform model compare reasonably well to those of the flight vehicle. These conclusions imply that complex, dynamic wind-tunnel testing might not be required to characterize ground effect for this particular configuration. Further research is recommended to identify configuration or flight condition parameters that indicate the presence of dynamic effects. Additional experimentation under controlled conditions with systematic variations in configuration parameters (such as leading-edge vortex strength, and so forth) and trajectory might lead to a satisfactory understanding of the DGE problem. The DGE wind-tunnel facility would be ideal for this purpose if the quality of the data obtained at comparatively higher dynamic rates could be improved.

Figure 15(b) shows the normalized lift coefficient data as a function of angle of attack. All constant-alpha approach flight data were obtained at angles of attack near 9°. Level pass maneuvers were conducted at angles of attack that ranged from 5 to 8°; however, results from each maneuver were adjusted to a reference angle of attack of 9° and an elevon position of 10° using free-stream derivatives, as previously discussed. These corrections (which are large compared to the corrections made to the constant-alpha method) further question the accuracy of the level pass maneuver data. In the wing planform results, no similar variation in angle of attack is observed.

Variations in the normalized lift coefficient as a function of elevon position are relatively small for the full-configuration tests (fig. 15(c)). All wing planform data were obtained at an elevon position of 10°, and the linear panel code data were independent of elevon position.

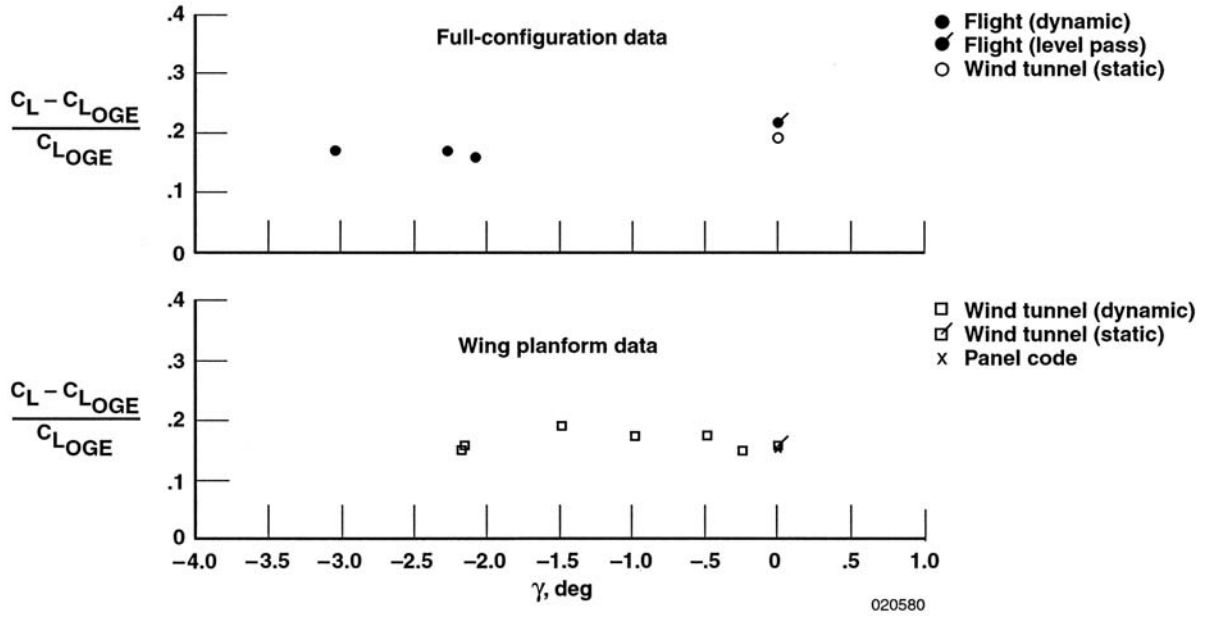

(a) Varying flightpath angle.

$9° \leq \alpha \leq 10°$.

$9° \leq \delta e \leq 10°$.

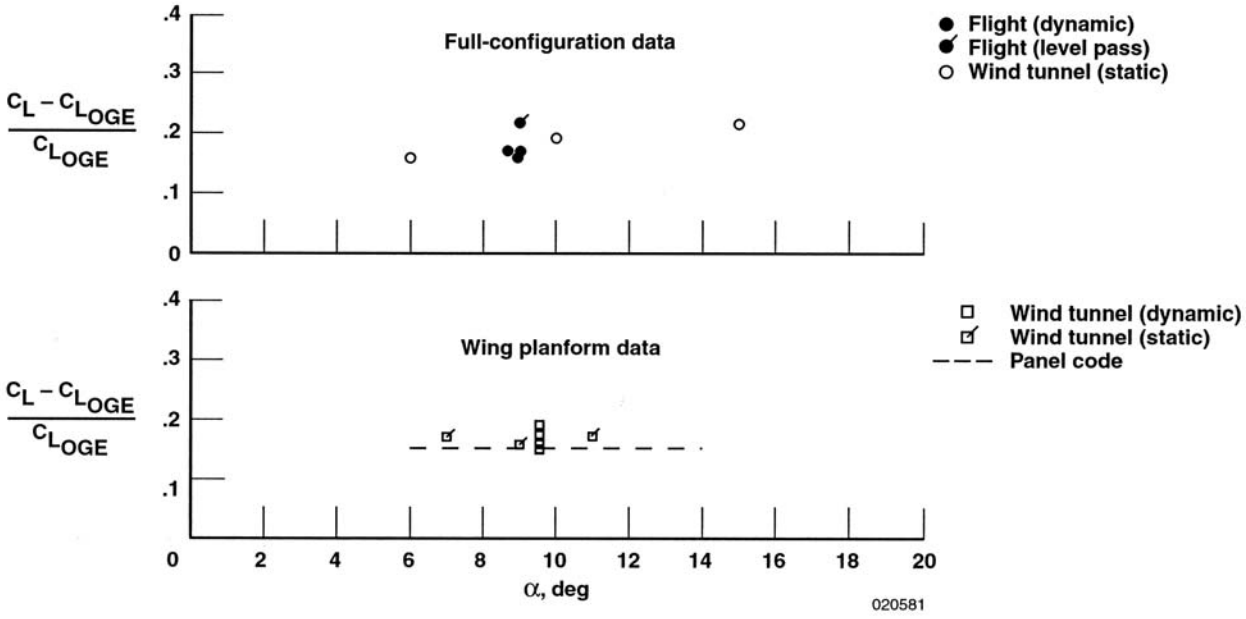

(b) Varying angle of attack and flightpath angle.

$9° \leq \delta e \leq 10°$.

Figure 15. Comparison of normalized ground-effect increments, *h/b*=0.3.

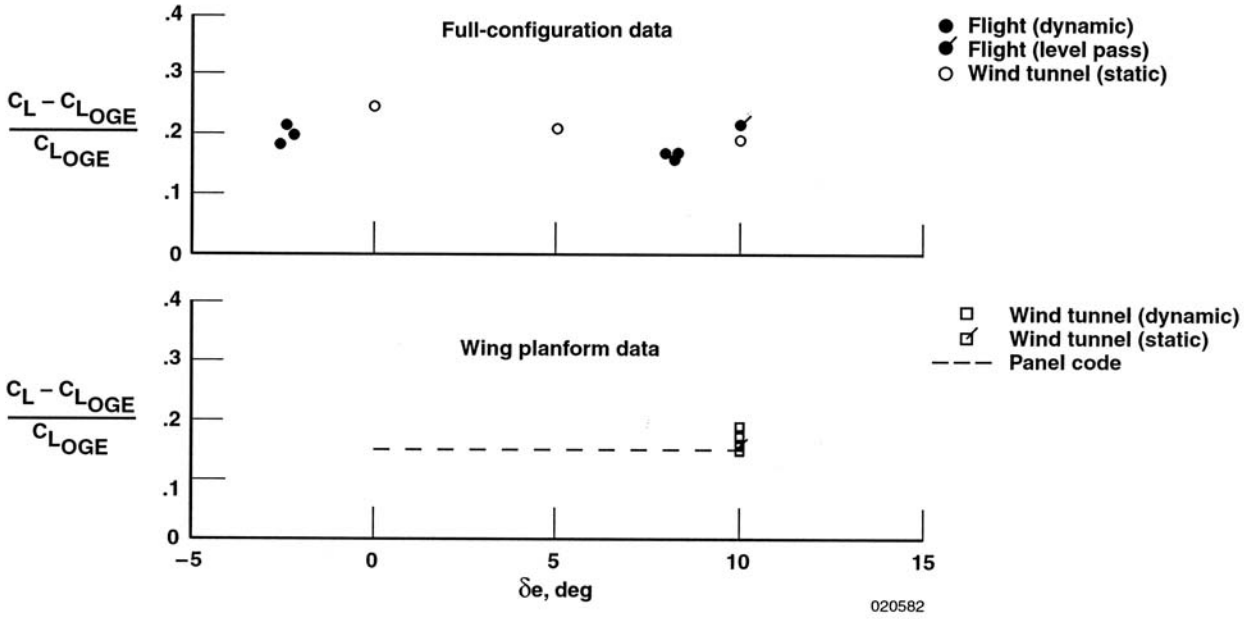

(c) Varying elevon position and flightpath angle.

$9° \leq \alpha \leq 10°$.

Figure 15. Concluded.

CONCLUDING REMARKS

Ground-effect characteristics of the Tu-144 supersonic transport airplane have been obtained from both dynamic and steady-state flight test maneuvers, and from a steady-state, full-configuration wind-tunnel test. A simple model of the Tu-144 wing planform was also tested under both dynamic and steady-state conditions using a developmental wind-tunnel model support system. Panel code predictions of ground effect for the wing planform were also obtained. Ground-effect increments from the various studies were compared by normalizing the coefficient data to out-of-ground effect (OGE) conditions and fitting the results to a power law trend.

Aerodynamic Findings

Results from the panel code analysis and steady-state wind-tunnel testing of both the full-configuration and wing planform models were found to be highly consistent and fit the power law relationship very well. Results from the dynamic flight tests, obtained during constant-alpha approaches, exhibited more scatter and some oscillatory trends, but these results compared favorably with the data from the steady-state, full-configuration wind-tunnel tests. Data from the steady-state flight tests, obtained during the level pass maneuvers, indicated slightly higher values of ground effect in the lift axis, but the data quality was relatively poor.

Data from the dynamic wind-tunnel tests were highly consistent for runs at low descent rates. The OGE data from these runs successfully matched the steady-state wind-tunnel data for the same model, further validating the dynamic test technique. Unfortunately, the effective flightpath angles for these runs were lower than those of the typical airplane landing flightpath. Data quality at higher descent rates was diminished by relatively large inertial forces, which complicated the balance measurements and limited the consistency of the model trajectory. Despite these limitations, the dynamic wind-tunnel tests indicated no significant variation in ground effect as a function of effective flightpath angle for this configuration. This finding conflicts with findings from previous studies of low-aspect-ratio, swept-wing configurations, which showed large differences between dynamic and static ground effect. Further research is recommended to identify controlling parameters that are responsible for these differences.

Test Technique Findings

The current dynamic wind-tunnel test data set presented in this report had several limitations, but this test technique might be highly valuable in future ground-effect research. In particular, the current data were obtained during pathfinder testing of the newly developed dynamic ground effect (DGE) model support system. Future improvements based on the current experience might lead to a capable system in terms of both operational effectiveness and test envelope. This type of system might be required to obtain parametric data to determine the controlling aspects of DGEs.

Although flight testing offers the only opportunity to validate ground-effect prediction methodologies, this type of measurement remains a challenging undertaking. The optimal flight test data in this study were obtained during constant-alpha approaches in which the results could be extracted from incremental changes from OGE reference conditions. Although 19 constant-alpha approaches were attempted, only 6 were acceptable for analysis. In future projects, more flight test time should be devoted to practicing and repeating the maneuvers to ensure a sufficient set of usable data. The level pass maneuvers required substantially more flight test time and were of limited value, primarily because of uncertainties in the determination of thrust variations between maneuvers.

REFERENCES

1. Nelson, C.P., “Effects Of Wing Planform On HSCT Off-Design Aerodynamics,” *10th Applied Aerodynamics Conference*, AIAA-92-2629, June 1992.

2. Kemp, William B., Vernard E. Lockwood, and W. Pelham Phillips, *Ground Effects Related to Landing of Airplanes With Low-Aspect-Ratio Wings*, NASA TN D-3583, Oct. 1966.

3. Snyder, C. Thomas, Fred J. Drinkwater III, and A. David Jones, *A Piloted Simulator Investigation of Ground Effect on the Landing Maneuver of a Large, Tailless, Delta-Wing Airplane*, NASA TN D-6046, Oct. 1970.

4. Anderson, John D., Jr., *Fundamentals of Aerodynamics*, McGraw-Hill Book Company, 1984.

5. Hedman, Sven G., *Vortex Lattice Method for Calculation of Quasi Steady State Loadings on Thin Elastic Wings in Subsonic Flow*, The Aeronautical Research Institute of Sweden, Report 105, 1966.

6. Chen, Yen-Sen and William G. Schweikhard, "Dynamic Ground Effects on a Two-Dimensional Flat Plate," *Journal of Aircraft,* vol. 22, no. 7, July 1985, pp. 638–640.

7. Nuhait, A.O., "Unsteady Ground Effects on Aerodynamic Coefficients of Finite Wings with Camber," *Journal of Aircraft*, vol. 32, no. 1, Jan.–Feb. 1995, pp. 186–192.

8. Nuhait, A.O. and M. F. Zedan, "Stability Derivatives of a Flapped Plate in Unsteady Ground Effect," *Journal of Aircraft,* vol. 32, no. 1, Jan.–Feb. 1995, pp. 124–129.

9. Chang, Ray Chung and Vincent U. Muirhead, "Effect of Sink Rate on Ground Effect of Low-Aspect-Ratio Wings," *Journal of Aircraft*, vol. 24, no. 3, March 1986, pp. 176–180.

10. Lee, Pai-Hung, C. Edward Lan, and Vincent U. Muirhead, *An Experimental Investigation of Dynamic Ground Effect*, NASA CR-4105, Dec. 1987.

11. Chang, Ray Chung, *An Experimental Investigation of Dynamic Ground Effect*, PhD Dissertation, University of Kansas, 1985.

12. Kemmerly, G.T., J.W. Paulson, Jr., and M. Compton, "Exploratory Evaluation of Moving-Model Technique for Measurement of Dynamic Ground Effects," *Journal of Aircraft*, vol. 25, no. 6, June 1988, pp. 557–562.

13. Kemmerly, Guy T. and John W. Paulson, Jr., *Investigation of a Moving-Model Technique for Measuring Ground Effects*, NASA TM-4080, Jan. 1989.

14. Paulson, John W., Jr., Guy T. Kemmerly, and William P. Gilbert, "Dynamic Ground Effects," *AGARD Fluid Dynamics Panel Symposium on Aerodynamics of Combat Aircraft Controls and of Ground Effects*, AGARD CP-465, April 1990, pp. 21-1–21-12.

15. Rolls, L. Stewart and David G. Koenig, *Flight-Measured Ground Effect on a Low-Aspect-Ratio Ogee Wing Including a Comparison with Wind-Tunnel Results*, NACA TN-D-3431, 1966.

16. Rolls, L. Stewart, C. Thomas Snyder, and William G Schweikhard, "Flight Studies of Ground Effects on Airplanes with Low-Aspect-Ratio Wings," *Conference on Aircraft Aerodynamics*, NASA SP-124, May 1966, pp. 285–295.

17. Baker, Paul A., William G. Schweikhard, and William R. Young, *Flight Evaluation of Ground Effect on Several Low-Aspect-Ratio Airplanes*, NASA TN D-6053, 1970.

18. Schweikhard, William, "A Method for In-Flight Measurement of Ground Effect on Fixed-Wing Aircraft," *Journal of Aircraft*, vol. 4, no. 2, Mar.–Apr. 1967, pp. 101–104.

19. Curry, Robert E., Bryan J. Moulton, and John Kresse, *An In-Flight Investigation of Ground Effect on a Forward-Swept Wing Airplane,* NASA TM-101708, Sept. 1989.

20. Corda, Stephen, Mark T. Stephenson, Frank W. Burcham, and Robert E. Curry, *Dynamic Ground Effects Flight Test of an F-15 Aircraft*, NASA TM-4604, Sept. 1994.

21. Curry, Robert E., *Dynamic Ground Effect for a Cranked Arrow Wing Airplane*, NASA TM-4799, Aug. 1997.

22. *Task 39 Tu-144LL Follow-on Program: Final Report*, HSR-AT Contract No. NAS1-20220, Submitted by The Boeing Company to NASA Langley Research Center, June 1999.

23. Cox, Timothy H. and Alisa Marshall, *Longitudinal Handling Qualities of the Tu-144LL Airplane and Comparisons With Other Large, Supersonic Aircraft,* NASA TM-2000-209020, May 2000.

24. Rivers, Robert A., E. Bruce Jackson, C. Gordon Fullerton, Timothy H. Cox, and Norman H. Princen, *A Qualitative Piloted Evaluation of the Tupolev Tu-144 Supersonic Transport*, NASA TM-2000-209850, Feb. 2000.

25. *Ashtech™ Precise Differential GPS Navigation (PNAV) Trajectory Software User's Guide*, Software Version 2.1.00-T, Document Number 600200, Revision B, May 1994.

26. Peñaranda, Frank E. and M. Shannon Freda, *Aeronautical Facilities Catalogue* (Volume 1), NASA RP-1132, 1985.

27. Graves, Sharon S., *Investigation of a Technique for Measuring Dynamic Ground Effect in a Subsonic Wind Tunnel*, NASA CR-1999-209544, Aug. 1999.

28. Hoerner, Sighard F. and Henry V. Borst, *Fluid-Dynamic Lift: Practical Information on Aerodynamic and Hydrodynamic Lift*, Second edition, Published by Mrs. Liselotte A. Hoerner, 1975.

REPORT DOCUMENTATION PAGE

Form Approved
OMB No. 0704-0188

1. AGENCY USE ONLY (Leave blank)	2. REPORT DATE	3. REPORT TYPE AND DATES COVERED
	October 2003	Technical Memorandum

4. TITLE AND SUBTITLE

Ground-Effect Characteristics of the Tu-144 Supersonic Transport Airplane

5. FUNDING NUMBERS

710-55-04-E8-RR-00-000

6. AUTHOR(S)

Robert E. Curry and Lewis R. Owens

7. PERFORMING ORGANIZATION NAME(S) AND ADDRESS(ES)

NASA Dryden Flight Research Center
P.O. Box 273
Edwards, California 93523-0273

8. PERFORMING ORGANIZATION REPORT NUMBER

H-2510

9. SPONSORING/MONITORING AGENCY NAME(S) AND ADDRESS(ES)

National Aeronautics and Space Administration
Washington, DC 20546-0001

10. SPONSORING/MONITORING AGENCY REPORT NUMBER

NASA/TM-2003-212035

11. SUPPLEMENTARY NOTES

12a. DISTRIBUTION/AVAILABILITY STATEMENT

Unclassified—Unlimited
Subject Category 02

This report is available at http://www.dfrc.nasa.gov/DTRS/

12b. DISTRIBUTION CODE

13. ABSTRACT (Maximum 200 words)

Ground-effect characteristics of the Tu-144 supersonic transport airplane have been obtained from flight and ground-based experiments to improve understanding of ground-effect phenomena for this class of vehicle. The flight test program included both dynamic measurements obtained during descending flight maneuvers and steady-state measurements obtained during level pass maneuvers over the runway. Both dynamic and steady-state wind-tunnel test data have been acquired for a simple planform model of the Tu-144 using a developmental model support system in the NASA Langley Research Center 14- by 22-ft Subsonic Wind Tunnel. Data from steady-state, full-configuration wind-tunnel tests of the Tu-144 are also presented. Results from the experimental methods are compared with results from simple computational methods (panel theory). A power law relationship has been shown to effectively fit the variation of lift with height above ground for all data sets. The combined data sets have been used to evaluate the test techniques and assess the sensitivity of ground effect to various parameters. Configuration details such as the fuselage, landing gear, canards, and engine flows have had little effect on the correlation between the various data sets. No distinct trend has been identified as a function of either flightpath angle or rate of descent.

14. SUBJECT TERMS	15. NUMBER OF PAGES
Aerodynamics, Flight test, Ground effect, Supersonic transport, Tu-144	42
	16. PRICE CODE

17. SECURITY CLASSIFICATION OF REPORT	18. SECURITY CLASSIFICATION OF THIS PAGE	19. SECURITY CLASSIFICATION OF ABSTRACT	20. LIMITATION OF ABSTRACT
Unclassified	Unclassified	Unclassified	Unlimited